GRAVITATIONAL WAVES FROM EARLY UNIVERSE TURBULENT SOURCES AT THE QCD SCALE

Emma Clarke
Carnegie Mellon University

Phys. Rev. D. 104 (2021) 4, 04513 (A. Brandenburg, EC, T. Kahniahsvili, Y. He)
Phys. Rev. Lett. 128, 221301 (2022) (T.K, EC, J. Stepp, AB)

PPC 2022

8 June 2022

EARLY UNIVERSE MAGNETIC FIELDS

Primordial magnetogenesis

- Inflation (Turner & Widrow 1998; Ratra 1992)
  - coupling of inflaton field to electromagnetic field
- Phase Transitions
  - Electroweak (EW). T ~ 100 GeV
  - QCD. T ~ 150 MeV
  - Types: 1st order (bubble collisions, Hogan 1983), Crossover

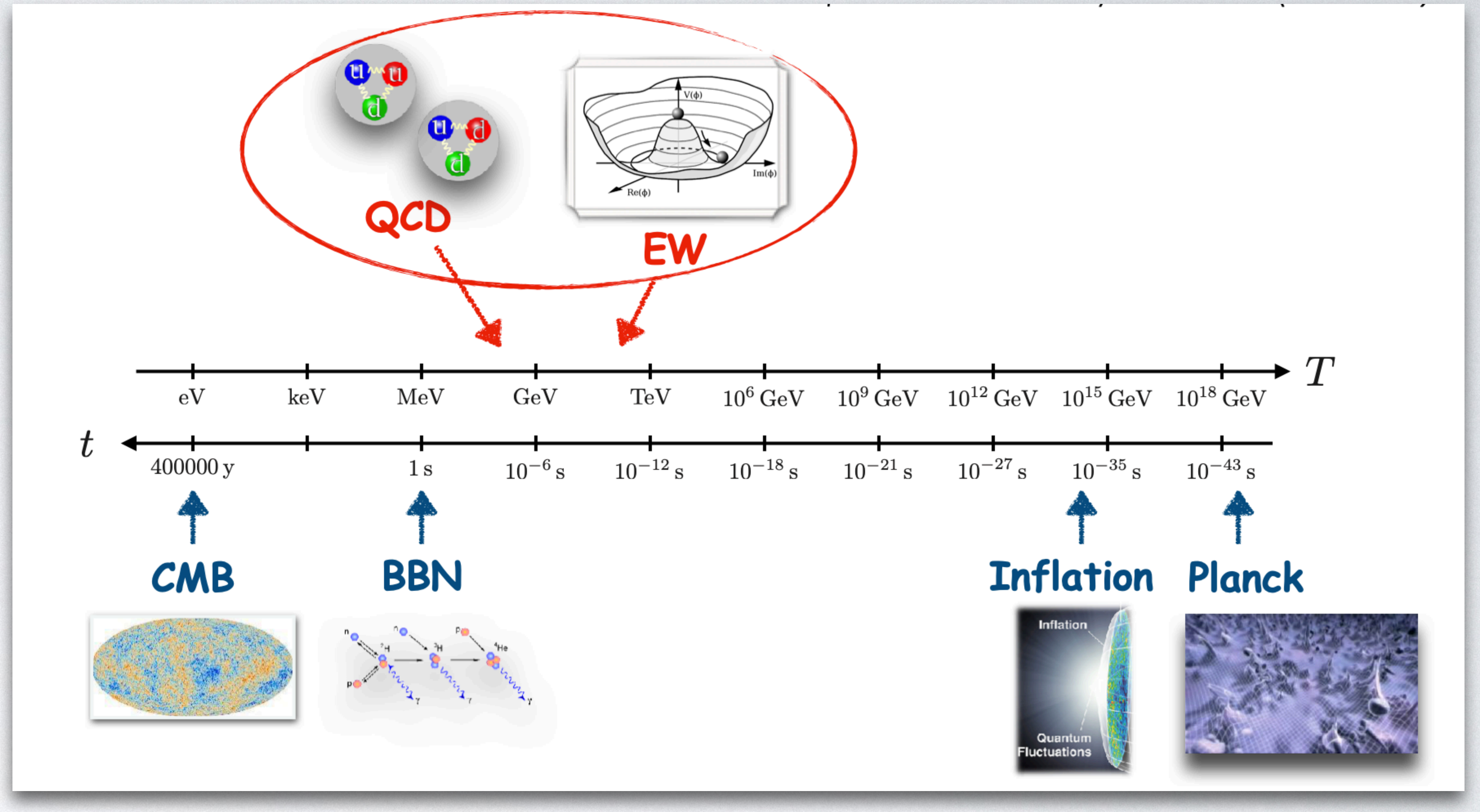

Magnetic Helicity

$$H_M = \int_V d^3\mathbf{r}\ \mathbf{A}\cdot\mathbf{B}$$

- related to parity violating process and beyond-SM physics
- *P* and *CP* violation can be related to processes giving rise to baryogenesis (Vachaspati 2001; Long, Sabancilar, Vachaspati 2014)
- leads to polarized GWs

first order transition

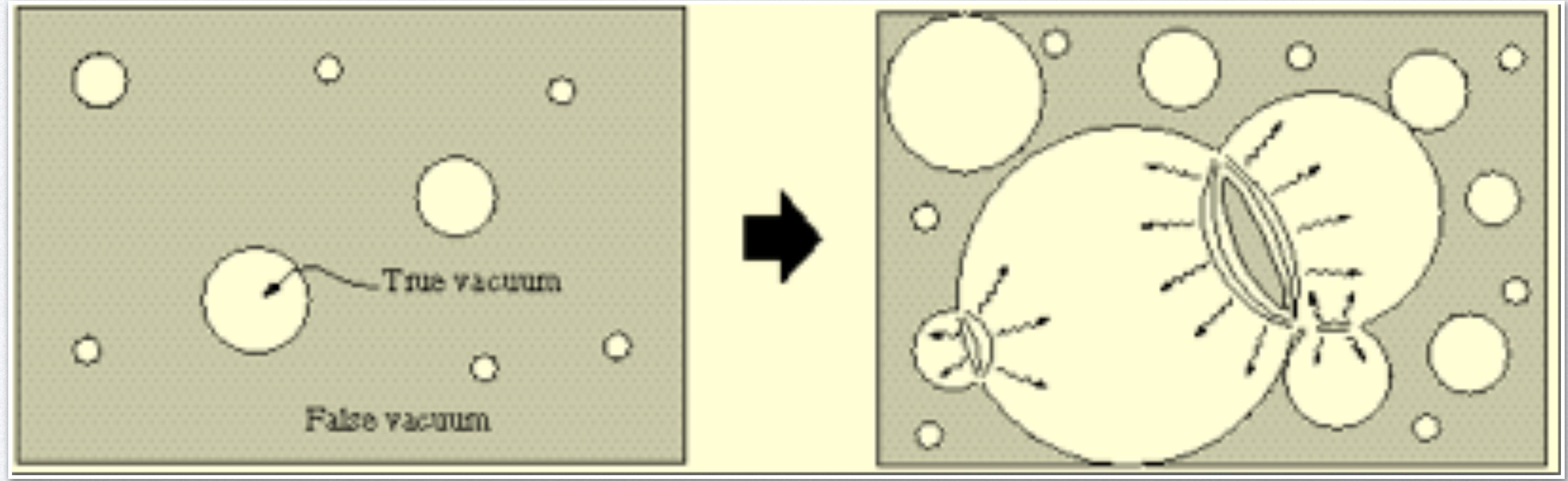

Cambridge CTC

GRAVITATIONAL WAVES

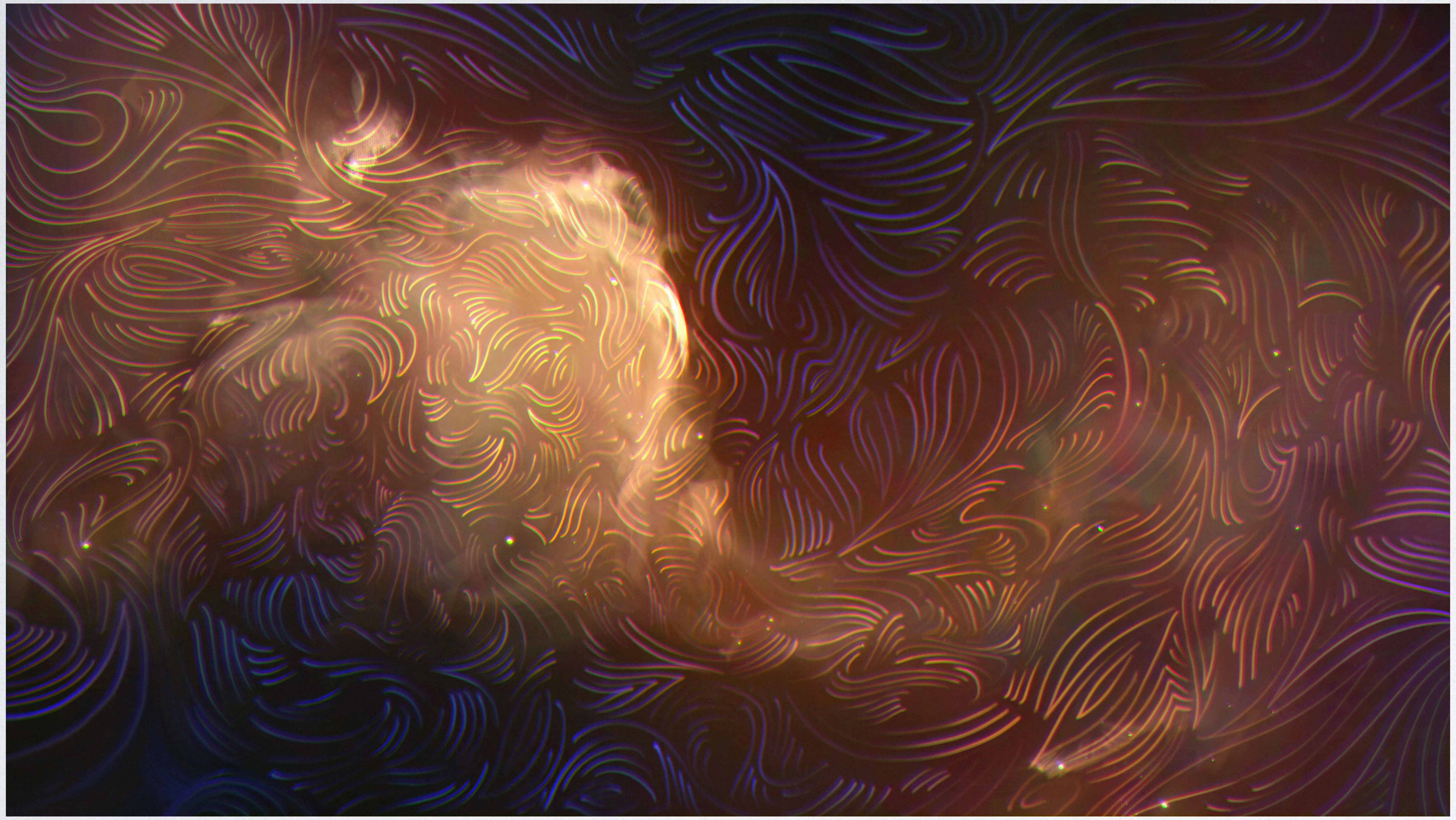

Quanta Magazine

Stress-energy tensor includes Reynolds and Maxwell stresses

$$T^{\mu\nu} = (p+\rho)U^{\mu}U^{\nu} + pg^{\mu\nu} + \frac{1}{4\pi}\left(F^{\mu\sigma}F^{\nu}{}_{\sigma} - \frac{1}{4}g^{\mu\nu}F_{\lambda\sigma}F^{\lambda\sigma}\right)$$

SVT decomposition: sources scalar (density), vector (vorticity), and tensor (gravitational wave) perturbations

- Brandenburg et al. CQG 38, 2021
- effects on CMB (Paoletti et al. MNRAS 2009 & refs within)

Gravitational waves (GW)

$$\left(\partial^2_{t_{\mathrm{phys}}} + 3H\partial_{t_{\mathrm{phys}}} - \nabla^2_{\mathrm{phys}}\right)h_{ij}^{\mathrm{phys}} = 16\pi G T^{\mathrm{TT}}_{ij,\mathrm{phys}}$$

GRAVITATIONAL WAVES

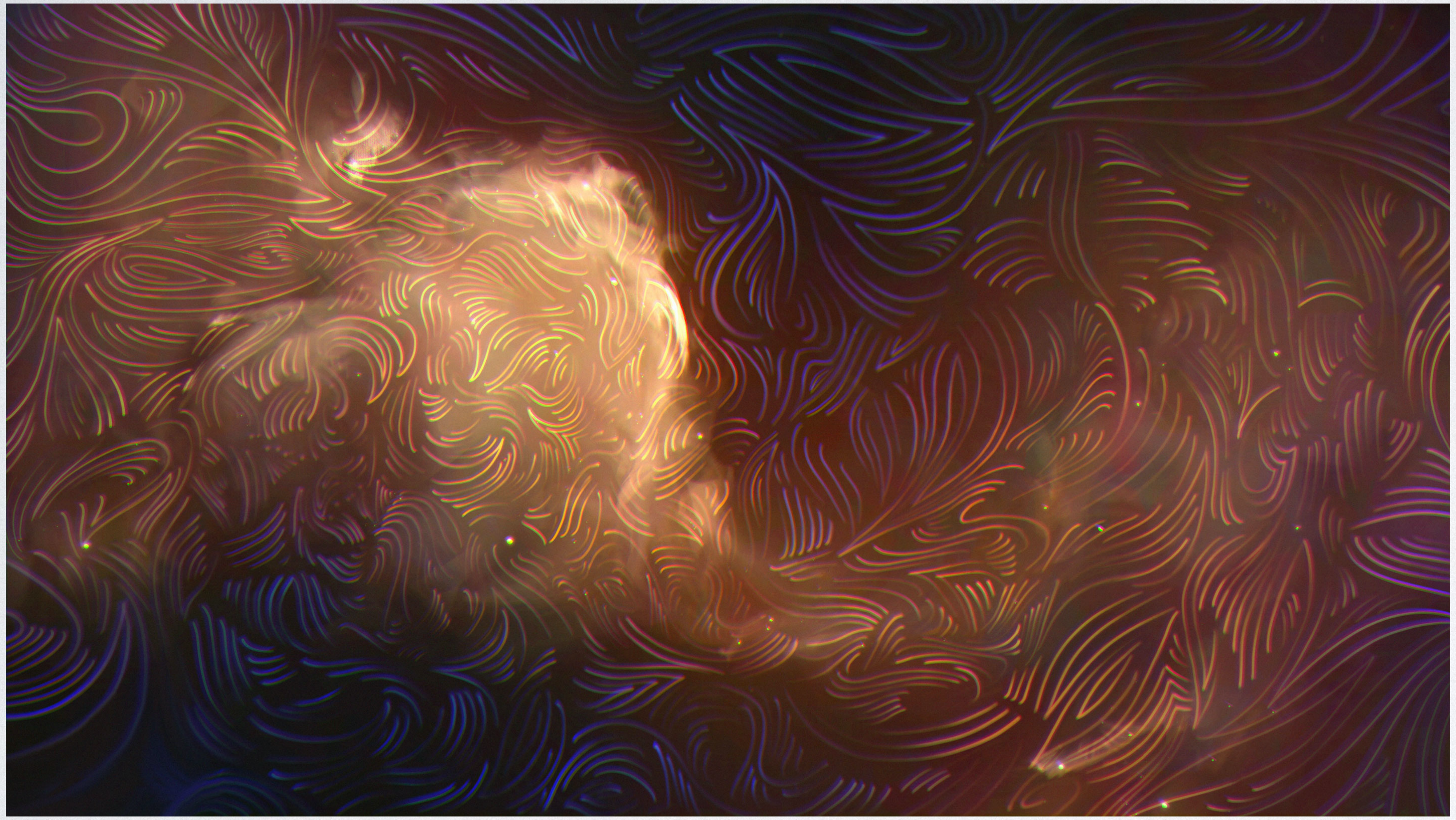

Quanta Magazine

Stress-energy tensor includes Reynolds and Maxwell stresses

$$T^{\mu\nu} = (p+\rho)U^{\mu}U^{\nu} + pg^{\mu\nu} + \frac{1}{4\pi}\left(F^{\mu\sigma}F^{\nu}{}_{\sigma} - \frac{1}{4}g^{\mu\nu}F_{\lambda\sigma}F^{\lambda\sigma}\right)$$

SVT decomposition: sources scalar (density), vector (vorticity), and tensor (gravitational wave) perturbations

- Brandenburg et al. CQG 38, 2021
- effects on CMB (Paoletti et al. MNRAS 2009 & refs within)

Gravitational waves (GW)

$$\left(\partial^2_{t_{\rm phys}} + 3H\partial_{t_{\rm phys}} - \nabla^2_{\rm phys}\right)h^{\rm phys}_{ij} = 16\pi G T^{\rm TT}_{ij,\rm phys}$$

stochastic source (turbulence)

stochastic background of gravitational waves

$$\Omega_{\rm GW}(f) = \frac{1}{\mathcal{E}_{\rm crit}(t)}\frac{{\rm d}\mathcal{E}_{\rm GW}}{{\rm d}\ln f}$$

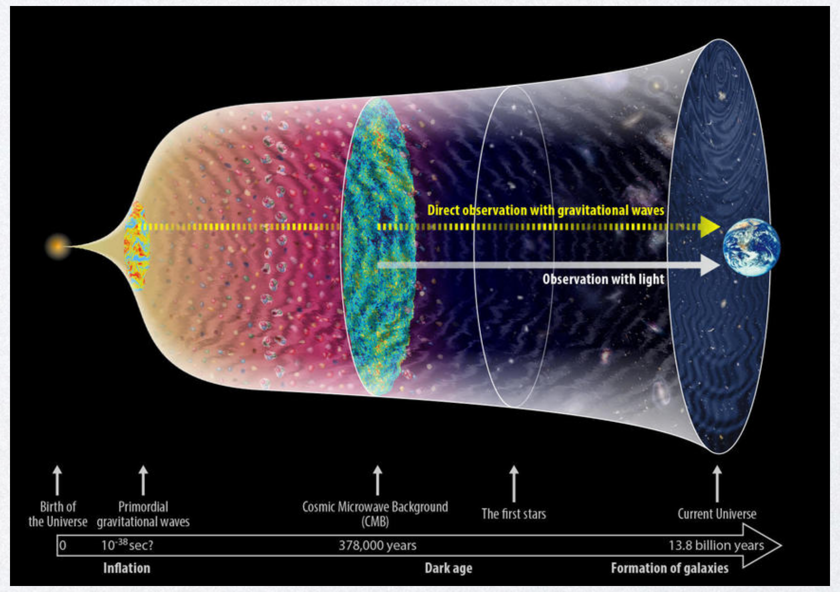

NOAJ

NUMERICAL SIMULATIONS

PENCIL CODE (https://github/com/pencil-code) used to solve the equations governing turbulent flows and GWs

- comoving variables, conformal time, normalized by values at generation

Hydromagnetic Equations

energy density

magnetic diffusivity

$$\frac{\partial \ln \rho}{\partial t} = -\frac{4}{3}\left(\boldsymbol{\nabla}\cdot\boldsymbol{u} + \boldsymbol{u}\cdot\boldsymbol{\nabla}\ln\rho\right) + \frac{1}{\rho}\left[\boldsymbol{u}\cdot(\boldsymbol{J}\times\boldsymbol{B}) + \eta\boldsymbol{J}^2\right]$$

$$\frac{\partial \boldsymbol{u}}{\partial t} = -\boldsymbol{u}\cdot\boldsymbol{\nabla}\boldsymbol{u} + \frac{\boldsymbol{u}}{3}\left(\boldsymbol{\nabla}\cdot\boldsymbol{u} + \boldsymbol{u}\cdot\boldsymbol{\nabla}\ln\rho\right) + \frac{2}{\rho}\boldsymbol{\nabla}\cdot(\rho\nu\mathbf{S})$$
$$-\frac{1}{4}\boldsymbol{\nabla}\ln\rho - \frac{\boldsymbol{u}}{\rho}\left[\boldsymbol{u}\cdot(\boldsymbol{J}\times\boldsymbol{B}) + \eta\boldsymbol{J}^2\right] + \frac{3}{4\rho}\boldsymbol{J}\times\boldsymbol{B}$$

kinematic viscosity

$$\frac{\partial \boldsymbol{B}}{\partial t} = \boldsymbol{\nabla}\times\left(\boldsymbol{u}\times\boldsymbol{B} - \eta\boldsymbol{J} + \boldsymbol{\mathcal{F}}\right), \quad \boldsymbol{J} = \boldsymbol{\nabla}\times\boldsymbol{B}$$

velocity (in units of c)

forcing term (forcing strength, helicity, vorticity, wavenumber)

current density

$$\boxed{\boldsymbol{\mathcal{F}}(\boldsymbol{x},t) = \mathrm{Re}[\mathcal{N}\tilde{\boldsymbol{f}}(\boldsymbol{k})\exp(i\boldsymbol{k}\cdot\boldsymbol{x} + i\varphi)]}$$

Gravitational Wave Equation

$$\left(\partial^2_{t_{\rm phys}} + 3H\partial_{t_{\rm phys}} - \boldsymbol{\nabla}^2_{\rm phys}\right)h^{\rm phys}_{ij} = 16\pi G \underbrace{T^{\rm TT}_{ij,\rm phys}}_{\text{MHD stresses}}$$

solve for comoving $h, \dot{h}$

$$\mathscr{E}_{\rm GW} \sim \left\langle \dot{h}^2 \right\rangle$$

$$\Omega_{\rm GW} \sim d\mathscr{E}_{\rm GW}/d\ln f$$

$$\mathscr{P}_{\rm GW}(k) = \frac{\left\langle h^*_+(\mathbf{k})h_+(\mathbf{k}') - h^*_-(\mathbf{k})h_-(\mathbf{k}')\right\rangle}{\left\langle h^*_+(\mathbf{k})h_+(\mathbf{k}') + h^*_-(\mathbf{k})h_-(\mathbf{k}')\right\rangle}$$

QCD SCALE

- Cosmological QCD transition: quark-gluon plasma (high temperature) to hadronic phase (lower temperature)

- Transition temperature T_* about150-200 MeV

- Degrees of freedom $g(T_*) \simeq g_S(T_*) \simeq 15$

- $f_* = \dfrac{a_* H_*}{a_0} \simeq (1.8 \times 10^{-8}\ \mathrm{Hz}) \left(\dfrac{g_*}{15}\right)^{1/6} \left(\dfrac{T_*}{150\ \mathrm{MeV}}\right)$
  →For small number of domains, frequency is in the sensitivity range of PTAs and astrometric missions

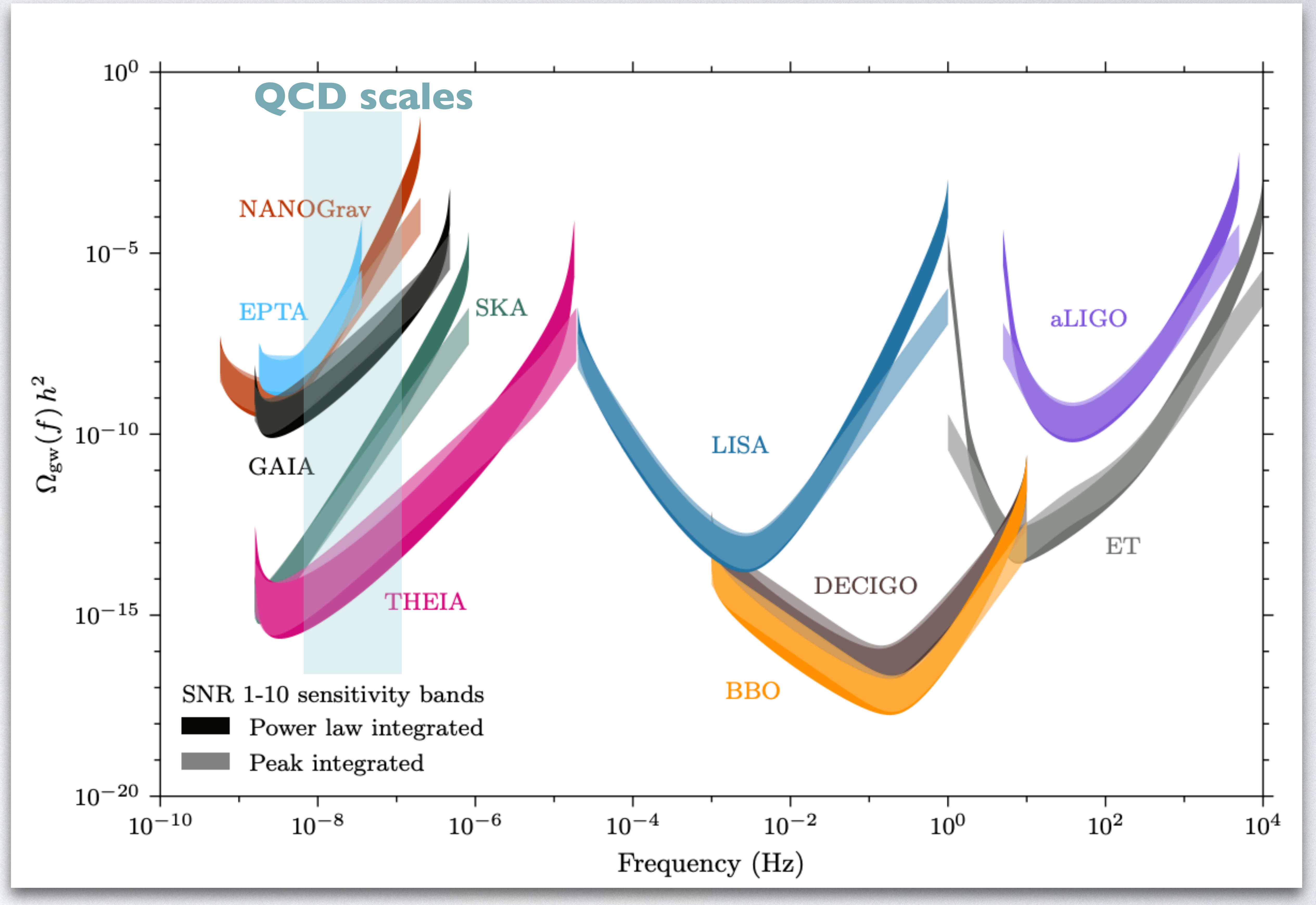

Garcia-Bellido, Murayama, White

NANOGRAV: DETECTING GWB WITH A PTA

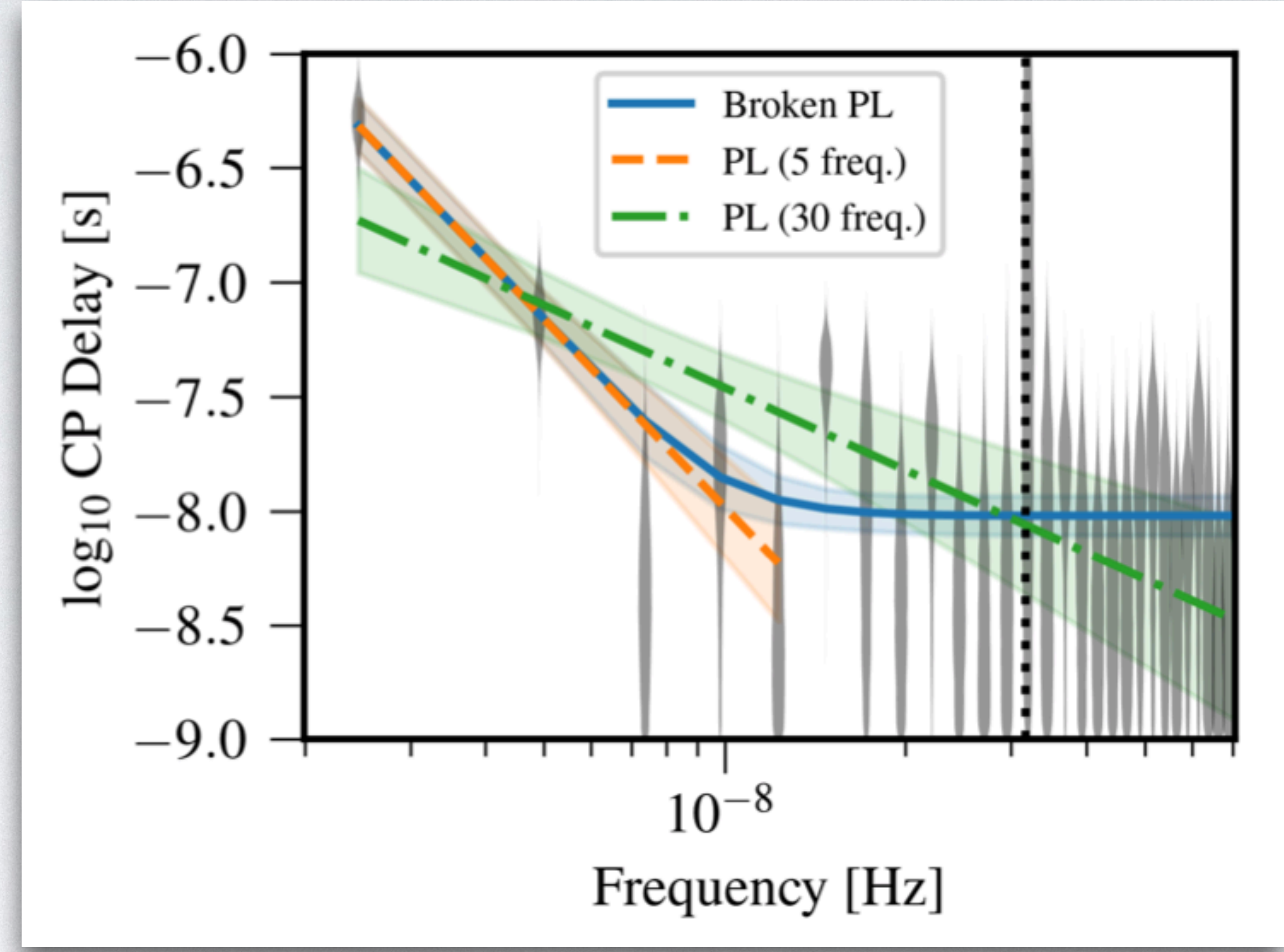

Arzoumanian et al (2020)

characteristic GW strain

$$h_c(f) = A_{\mathrm{CP}}\left(\frac{f}{f_{\mathrm{yr}}}\right)^{(3-\gamma_{\mathrm{CP}})/2}$$

GW energy density spectrum

$$\Omega_{\mathrm{GW}}(f) = \frac{1}{\mathscr{E}_{\mathrm{crit}}(t)}\frac{\mathrm{d}\mathscr{E}_{\mathrm{GW}}}{\mathrm{d}\ln f}$$

$$= \frac{2\pi^2}{3H_0^2} f^2 h_c^2(f)$$

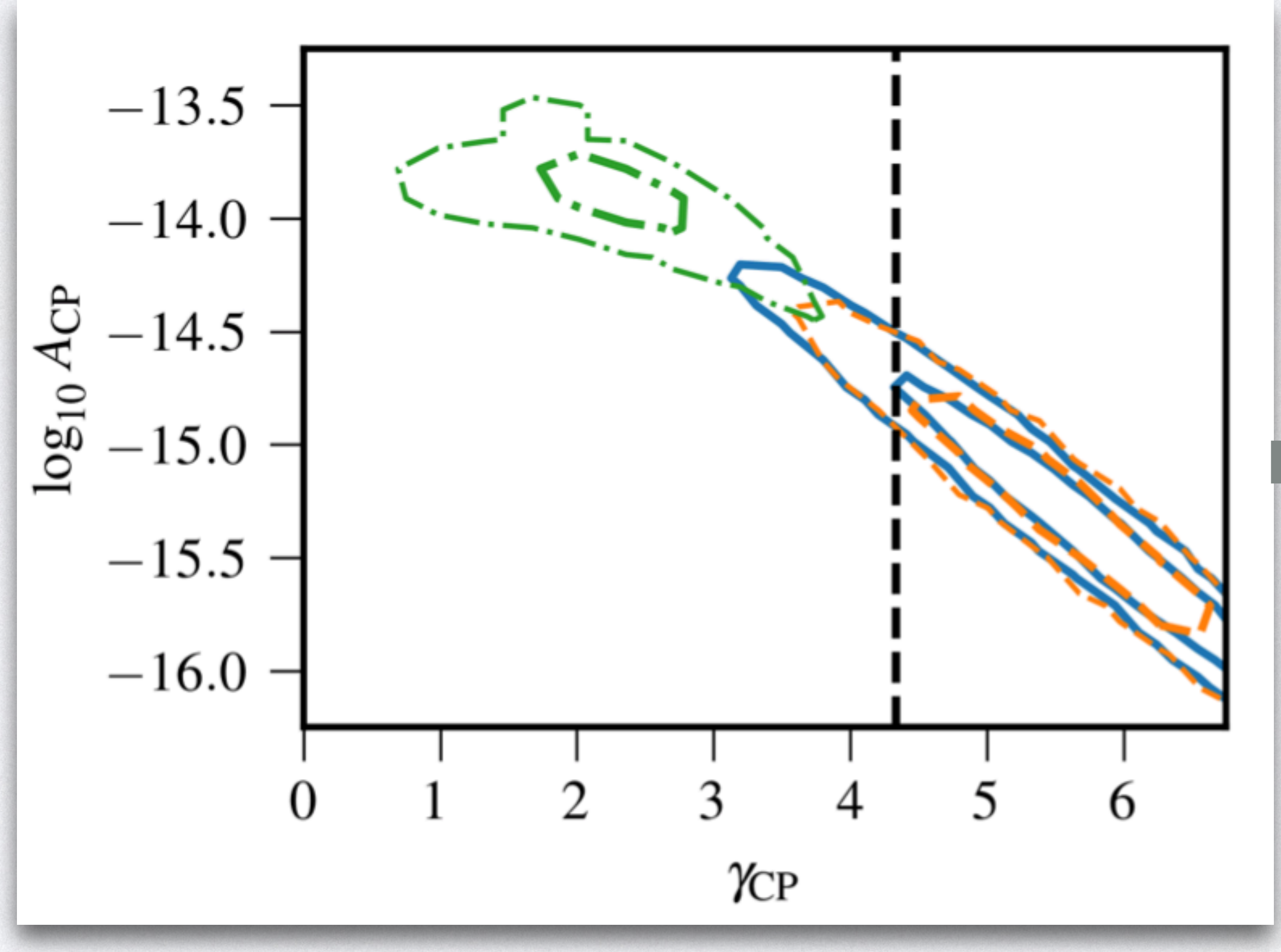

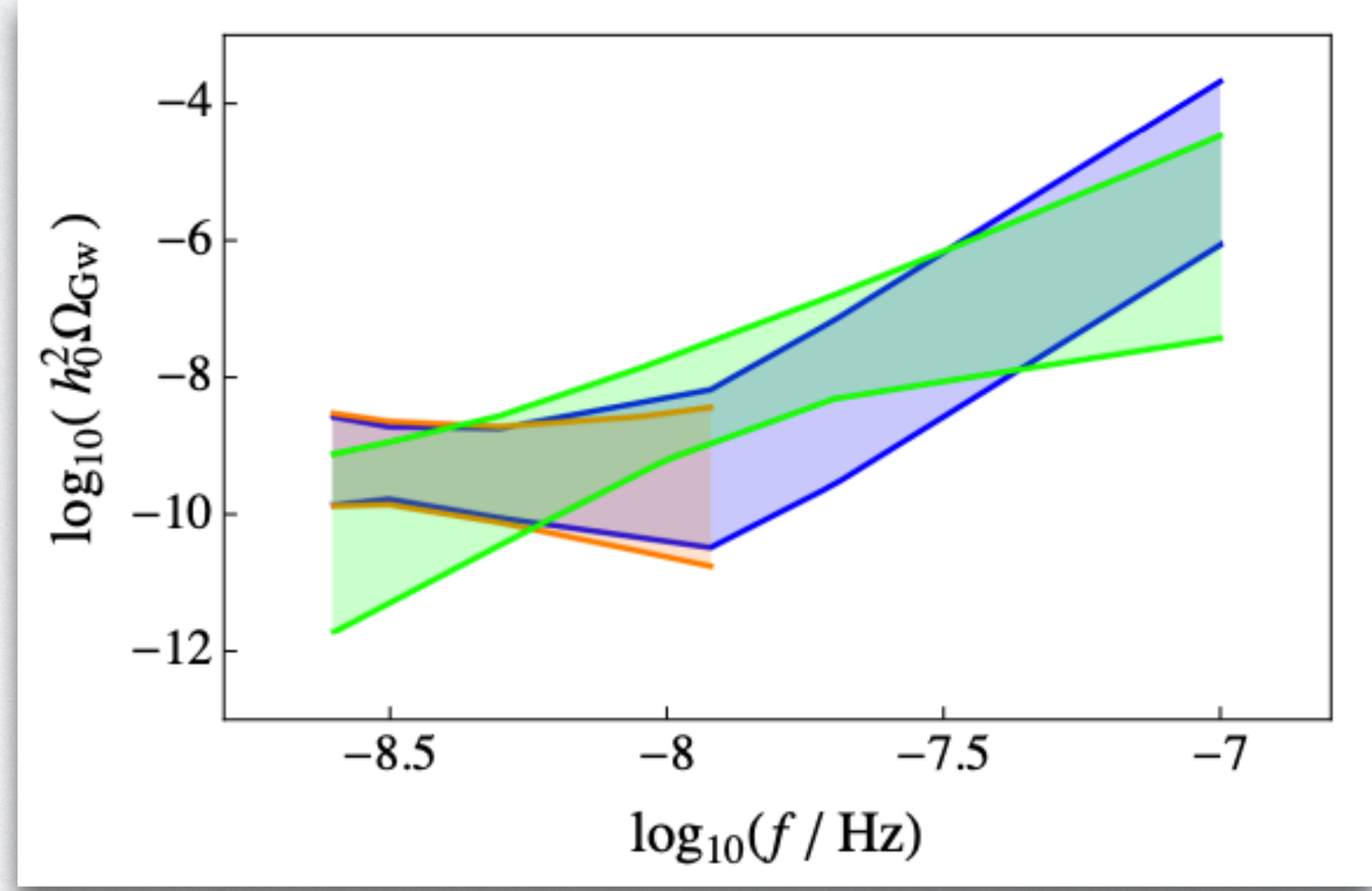

NANOGrav frequency sensitivity range

12.5yr results

common spectrum process ✔

quadrupolar spatial correlations ?

ASTROMETRY

- Astrometry: measuring the apparent positions of stars
- GAIA: large surveys of stars, monitor position of sources in the sky
- Detecting GWs:
    - GWs affect the propagation of light causing the apparent position of objects on the sky to change with time
    - GWs affect the apparent position of a star: multiple subsequent measurements of the same star can be used to turn GAIA into a GW observatory
- GAIA might complement PTAs at high galactic latitudes as well as high frequencies

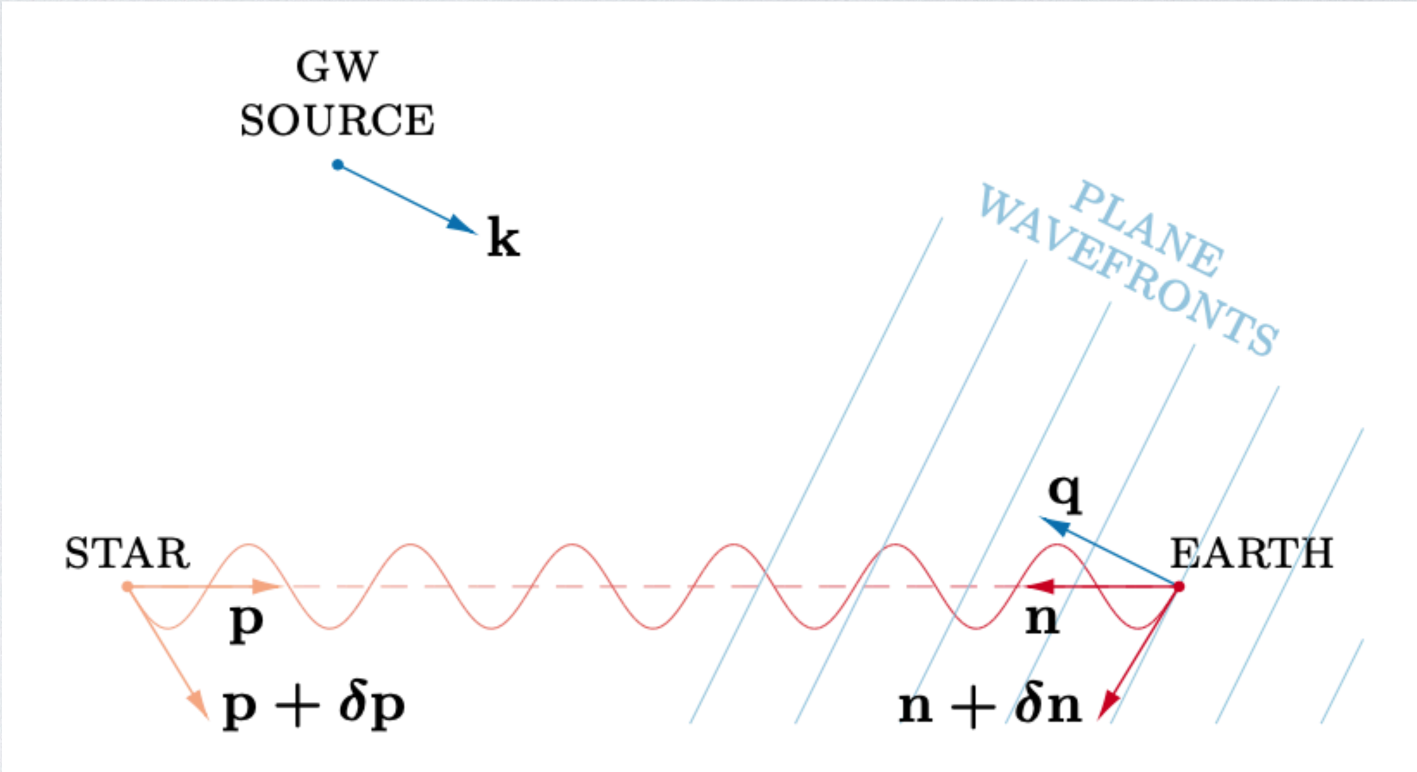

Mihaylov et al. 2018

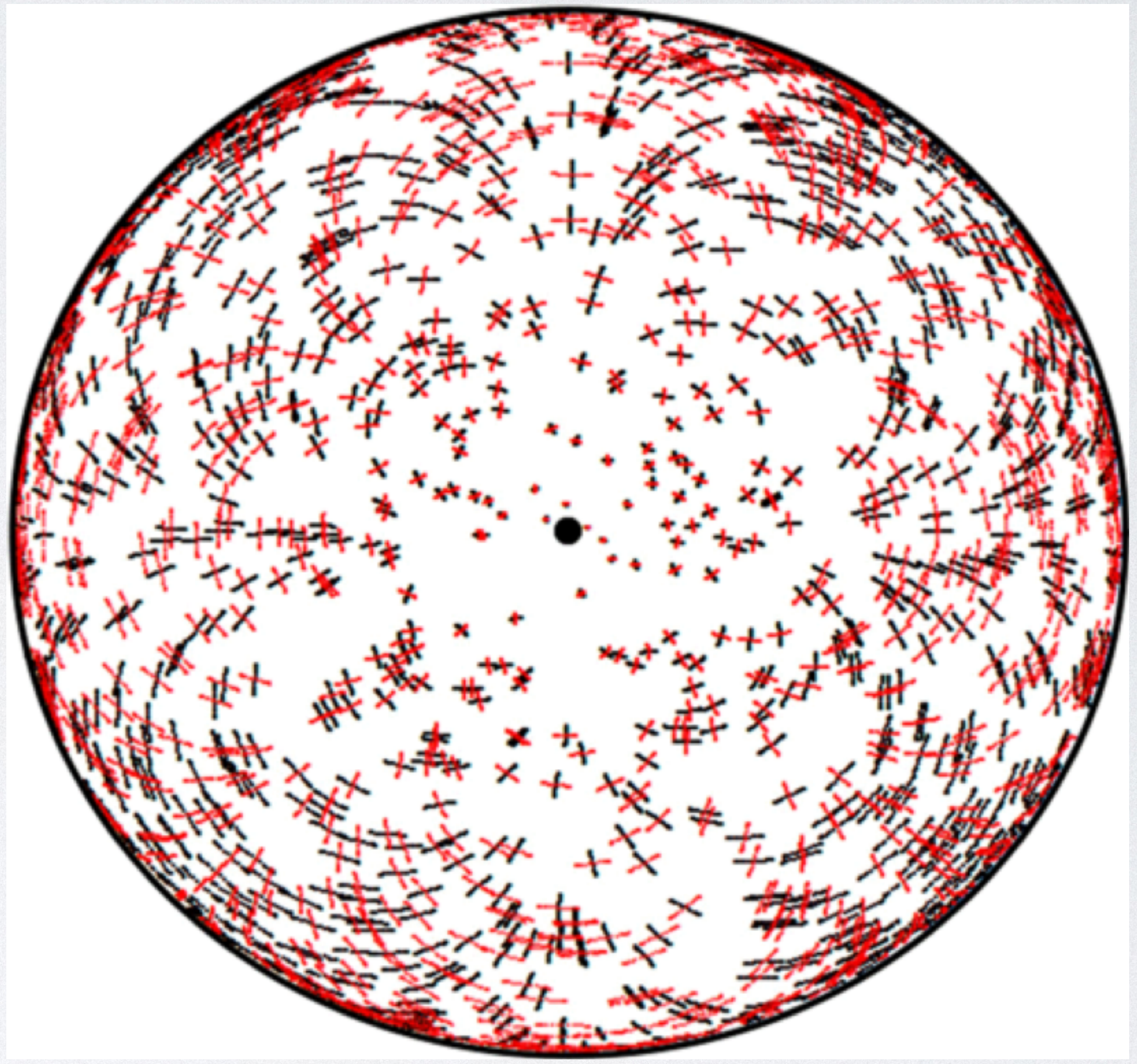

Astrometric response to a GW coming from the sky location marked with the black dot (center). GW causes stars to oscillate at the GW frequency. The black (red) lines show movement tracks for a linearly plus (cross) polarised GW. (Moore et al. 2017)

MAGNETIC FIELD BOUNDS

Correlation length of magnetic field $\xi_{M*} \leq \lambda_{H*} = (a_* H_*)^{-1}$

Field Strength

- BBN constrains $N_{\rm eff} = \underbrace{N_{\rm eff}^{(\nu)}}_{N_{\rm eff}^{(\nu)}=3.046 \text{ Standard Model}} + \underbrace{\Delta N_{\rm eff}}_{\text{additional relativistic components}}$
- $N_{\rm eff} = 3.168$, $\Delta N_{\rm eff} = 0.122$ (95% confidence interval upper bound, Fields et al. 2020; CMB + light element abundances)
- Constrains energy density in extra relativistic components

$$\frac{\rho_B}{\rho_\gamma} = \frac{7}{8}\left(\frac{4}{11}\right)^{4/3} \Delta N_{\rm eff} = 0.028$$

➡$B_{\rm BBN}^{\rm max} = 6.2 \times 10^{-7}$ G

ENERGY DENSITY

driving

non helical (p≃1 typical)

driving

helical (p = 2/3)

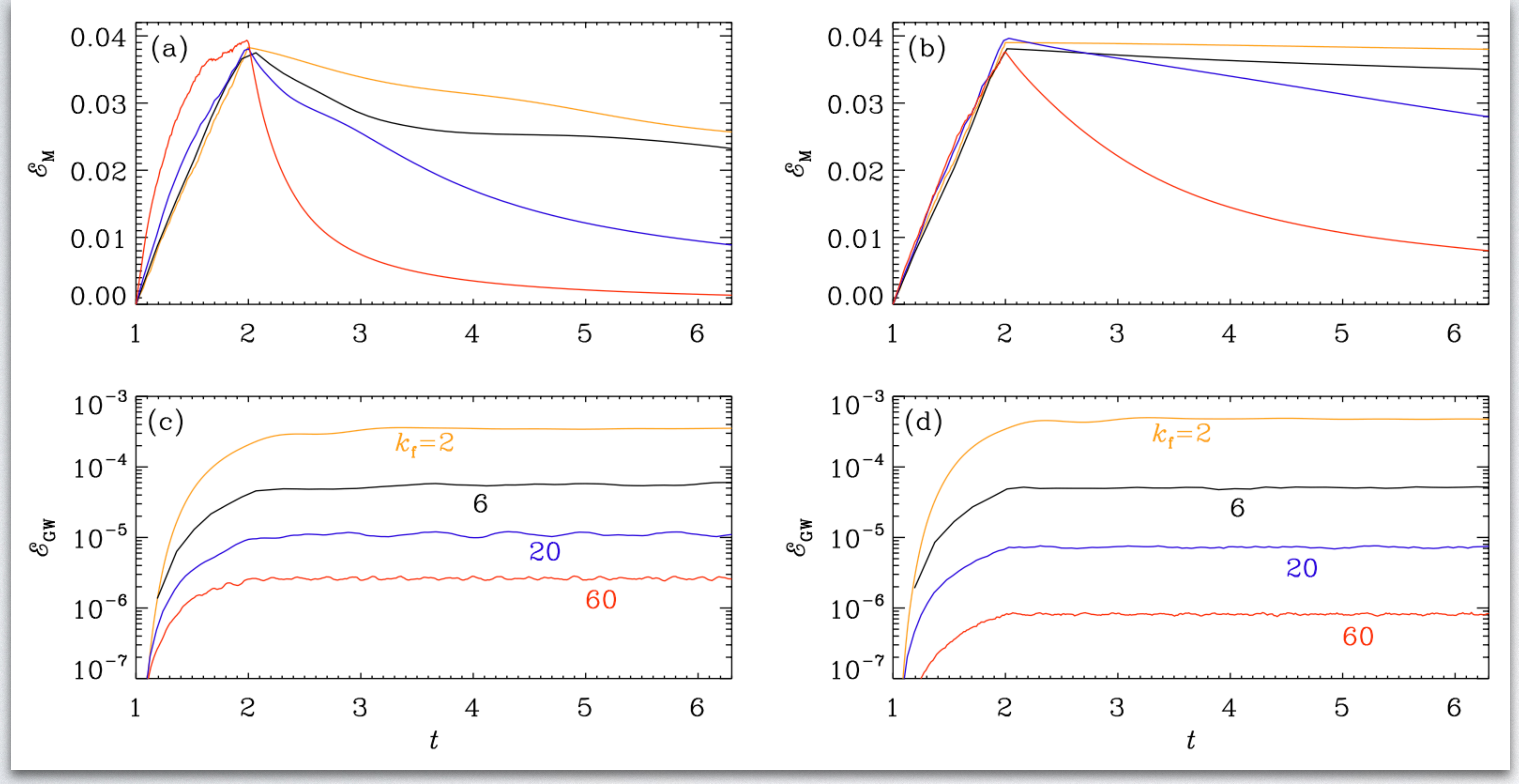

magnetic energy density

$$\mathcal{E}_\mathrm{M} \sim \langle \mathbf{B}^2 \rangle$$

peak value $\mathcal{E}_\mathrm{M}^\mathrm{max}$

turbulent decay

$$\mathcal{E}_\mathrm{M}(t) \sim t^{-p}$$

energy density carried by GWs

$$\mathcal{E}_\mathrm{GW} \sim \langle \dot{h}^2 \rangle$$

saturates at $\mathcal{E}_\mathrm{GW}^\mathrm{sat}$

$$\mathcal{E}_\mathrm{GW}^\mathrm{sat} = (q\mathcal{E}_\mathrm{M}^\mathrm{max}/k_\mathrm{f})^2$$

with $q = 1.1$

NON HELICAL VS HELICAL SPECTRA

$$\Omega_{\rm GW}(t,f) = \frac{1}{\mathcal{E}_{\rm crit}(t)}\frac{d\mathcal{E}_{\rm GW}}{d\ln f}$$

$$\Omega_{\rm GW}(t_0,f) = \left(\frac{a_*}{a_0}\right)^4 \left(\frac{H_*}{H_0}\right)^2 \Omega_{\rm GW}(t_*,f)$$

non helical

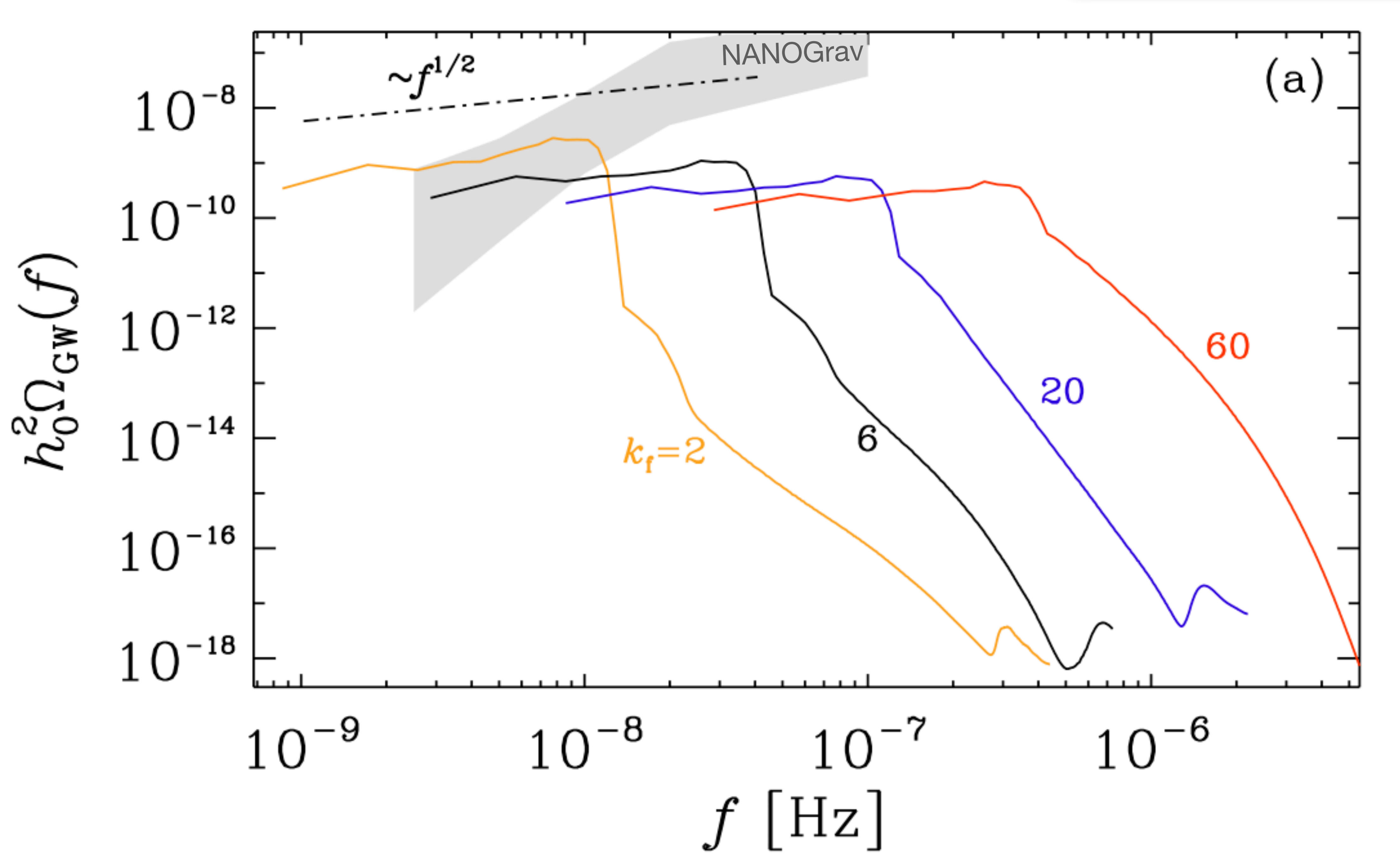

Run	k_f	k_1	f_0	p	τ	$\mathcal{E}_{\rm M}^{\rm max}$	$\mathcal{E}_{\rm GW}^{\rm sat}$	$h_{\rm rms}^{\rm sat}$	B [μG]	$h_0^2\Omega_{\rm GW}(f)$	h_c
noh1	2	0.3	1.9×10^{-1}	1.0	16	3.83×10^{-2}	3.53×10^{-4}	4.83×10^{-2}	0.78	1.09×10^{-8}	4.83×10^{-14}
noh2	6	1	6.0×10^{-2}	1.0	4.5	3.75×10^{-2}	5.61×10^{-5}	7.06×10^{-3}	0.78	1.73×10^{-9}	7.07×10^{-15}
noh3	20	3	2.3×10^{-2}	1.3	2.0	3.81×10^{-2}	1.11×10^{-5}	1.15×10^{-3}	0.78	3.44×10^{-10}	1.15×10^{-15}
noh4	60	10	1.0×10^{-2}	1.4	0.43	3.93×10^{-2}	2.62×10^{-6}	1.65×10^{-4}	0.79	8.10×10^{-11}	1.65×10^{-16}

helical

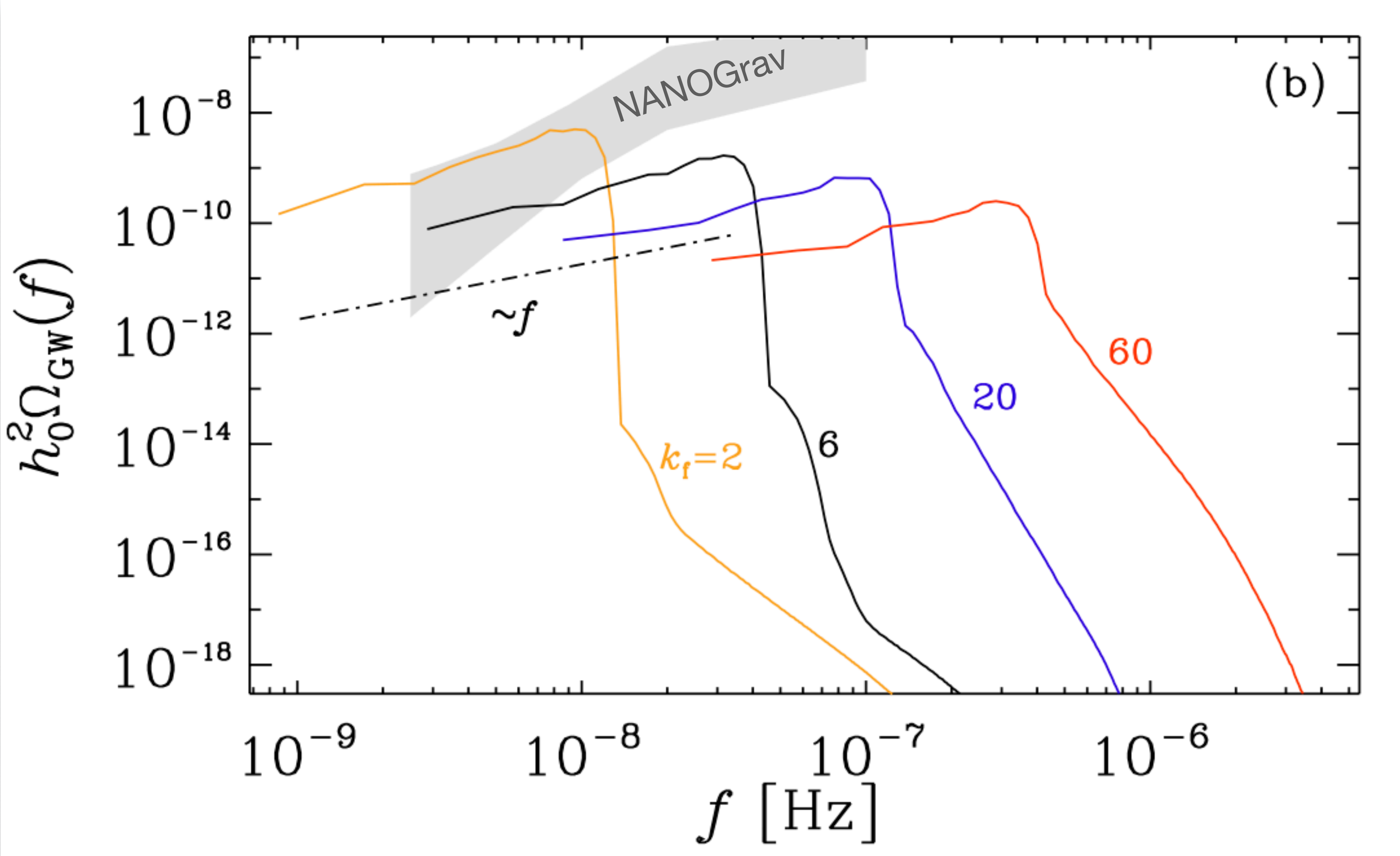

Run	k_f	k_1	f_0	p	τ	$\mathcal{E}_{\rm M}^{\rm max}$	$\mathcal{E}_{\rm GW}^{\rm sat}$	$h_{\rm rms}^{\rm sat}$	B [μG]	$h_0^2\Omega_{\rm GW}(f)$	h_c
hel1	2	0.3	1.9×10^{-1}	0.67	100	3.90×10^{-2}	4.85×10^{-4}	4.33×10^{-2}	0.79	1.50×10^{-8}	4.33×10^{-14}
hel2	6	1	5.6×10^{-2}	0.67	20	3.81×10^{-2}	5.05×10^{-5}	4.69×10^{-3}	0.78	1.56×10^{-9}	4.69×10^{-15}
hel3	20	3	2.0×10^{-2}	0.67	4.0	3.96×10^{-2}	7.26×10^{-6}	6.66×10^{-4}	0.80	2.24×10^{-10}	6.66×10^{-16}
hel4	60	10	6.5×10^{-3}	0.67	0.50	3.76×10^{-2}	8.15×10^{-7}	7.18×10^{-5}	0.78	2.52×10^{-11}	7.18×10^{-17}

MAGNETIC FIELD BOUNDS

Correlation length of magnetic field $\xi_{M*} \leq \lambda_{H*} = (a_* H_*)^{-1}$

Field Strength

- BBN constrains $N_{\mathrm{eff}} = \underbrace{N_{\mathrm{eff}}^{(\nu)}}_{\substack{N_{\mathrm{eff}}^{(\nu)} = 3.046 \\ \text{Standard Model}}} + \underbrace{\Delta N_{\mathrm{eff}}}_{\substack{\text{additional relativistic} \\ \text{components}}}$

- $N_{\mathrm{eff}} = 3.168$, $\Delta N_{\mathrm{eff}} = 0.122$ (95% confidence interval upper bound, Fields et al. 2020; CMB + light element abundances)

- Constrains energy density in extra relativistic components

$$\frac{\rho_B}{\rho_\gamma} = \frac{7}{8}\left(\frac{4}{11}\right)^{4/3} \Delta N_{\mathrm{eff}} = 0.028$$

➡ $B_{\mathrm{BBN}}^{\mathrm{max}} = 6.2 \times 10^{-7}$ G

MAGNETIC FIELD BOUNDS

Correlation length of magnetic field $\xi_{M*} \leq \lambda_{H*} = (a_* H_*)^{-1}$

Field Strength

- BBN constrains $N_{\rm eff} = \underbrace{N_{\rm eff}^{(\nu)}}_{\substack{N_{\rm eff}^{(\nu)}=3.046 \\ \text{Standard Model}}} + \underbrace{\Delta N_{\rm eff}}_{\substack{\text{additional relativistic} \\ \text{components}}}$

- $N_{\rm eff} = 3.168$, $\Delta N_{\rm eff} = 0.122$ (95% confidence interval upper bound, Fields et al. 2020; CMB + light element abundances)

- Constrains energy density in extra relativistic components

$$\left.\frac{\rho_B}{\rho_\gamma}\right|_{\rm T_{BBN}} = \frac{7}{8}\left(\frac{4}{11}\right)^{4/3} \Delta N_{\rm eff} = 0.028$$

$$\Rightarrow \left. B_{\rm BBN}^{\max}\right|_{\rm T_{BBN}} = 6.2 \times 10^{-7}\,\mathrm{G} \text{ and turbulence decay allows } B_*^{\max} > B_{\rm BBN}^{\max}$$

GW SPECTRA: QCD SCALE

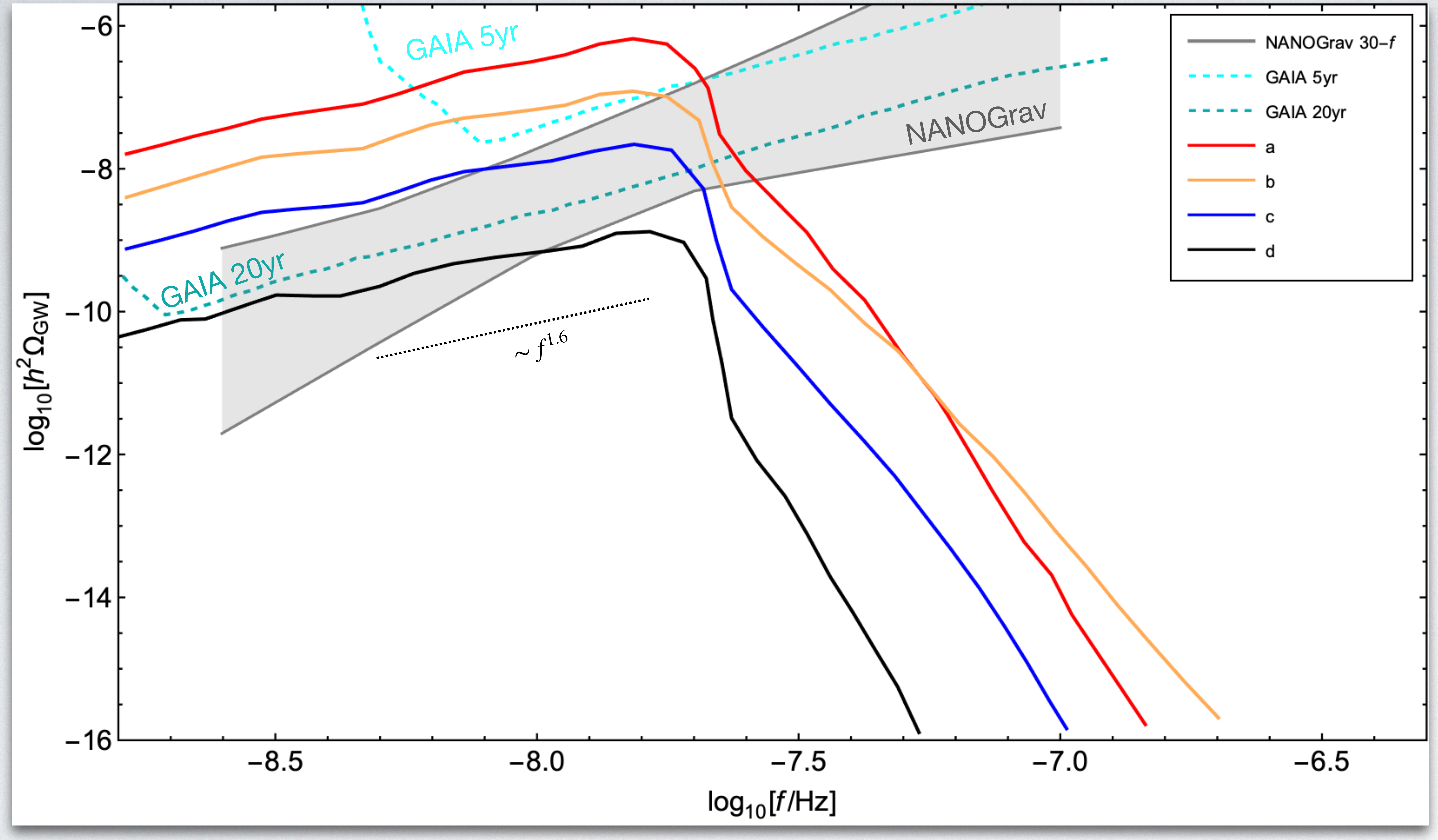

QCD Scale Runs: a-d
(below peak $\Omega_{GW} \sim f^{1.6}$)

NANOGrav 12.5-yr Results
(fit to 30-frequency bins)
[Arzoumanian et al. 2020]

GAIA Sensitivity Curves
(mission time)
[Moore et al. 2017]

decreasing f_0

Run	f_0	ν	$\mathcal{E}_{\mathrm{M}}^{\max}$	$\mathcal{E}_{\mathrm{GW}}^{\mathrm{sat}}$	$h_{\mathrm{rms}}^{\mathrm{sat}}$	B_{rms} [μG]	$h_0^2\Omega_{\mathrm{GW}}$	h_c
a	5×10^{-1}	2×10^{-2}	1.40×10^{-0}	2.6×10^{-1}	2.7×10^{-1}	4.7	8.04×10^{-6}	2.69×10^{-13}
a2	3×10^{-1}	2×10^{-2}	5.08×10^{-1}	3.0×10^{-2}	9.2×10^{-2}	2.9	9.19×10^{-7}	9.19×10^{-14}
b	3×10^{-1}	5×10^{-3}	9.40×10^{-1}	5.4×10^{-2}	1.4×10^{-1}	3.9	1.66×10^{-6}	1.36×10^{-13}
c	2×10^{-1}	5×10^{-3}	4.26×10^{-1}	9.4×10^{-3}	5.7×10^{-2}	2.6	2.90×10^{-7}	5.73×10^{-14}
d	1×10^{-1}	5×10^{-3}	1.09×10^{-1}	5.5×10^{-4}	1.4×10^{-2}	1.3	1.71×10^{-8}	1.38×10^{-14}

GW POLARIZATION SPECTRA

<u>circular polarization degree</u>

helical (antisymmetric) energy spectrum

$$\mathscr{P}(k) = \frac{\left\langle h_+^*(\mathbf{k})h_+(\mathbf{k}') - h_-^*(\mathbf{k})h_-(\mathbf{k}')\right\rangle}{\left\langle h_+^*(\mathbf{k})h_+(\mathbf{k}') + h_-^*(\mathbf{k})h_-(\mathbf{k}')\right\rangle} = \frac{\mathscr{H}(k)}{H(k)}$$

energy spectrum

- Retains information about the initial fractional helicity of source (Kahniashvili et al. 2021)

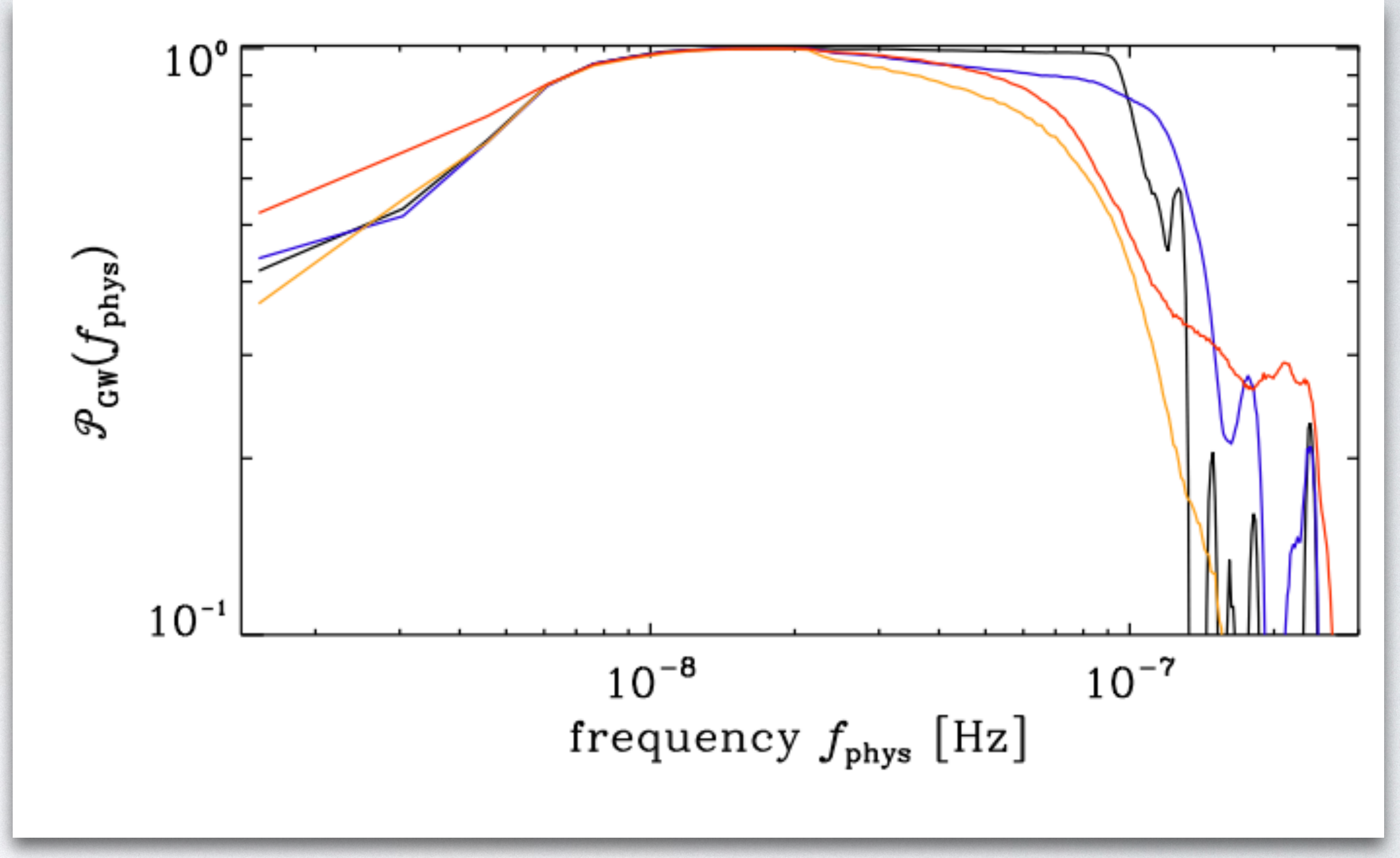

Run	f_0	ν
a	5×10^{-1}	2×10^{-2}
a2	3×10^{-1}	2×10^{-2}
b	3×10^{-1}	5×10^{-3}
c	2×10^{-1}	5×10^{-3}
d	1×10^{-1}	5×10^{-3}

GW POLARIZATION SPECTRA

Detection

- PTAs: more pulsars (≥ 100), SNR(≥ 400) (Belgacem + Kamionkowski 2021); solar system proper motion (Seto 2006+2007; applied to LISA in Domcke et al 2020)

- Astrometry: project with Deyan Mihaylov & Guotong Sun

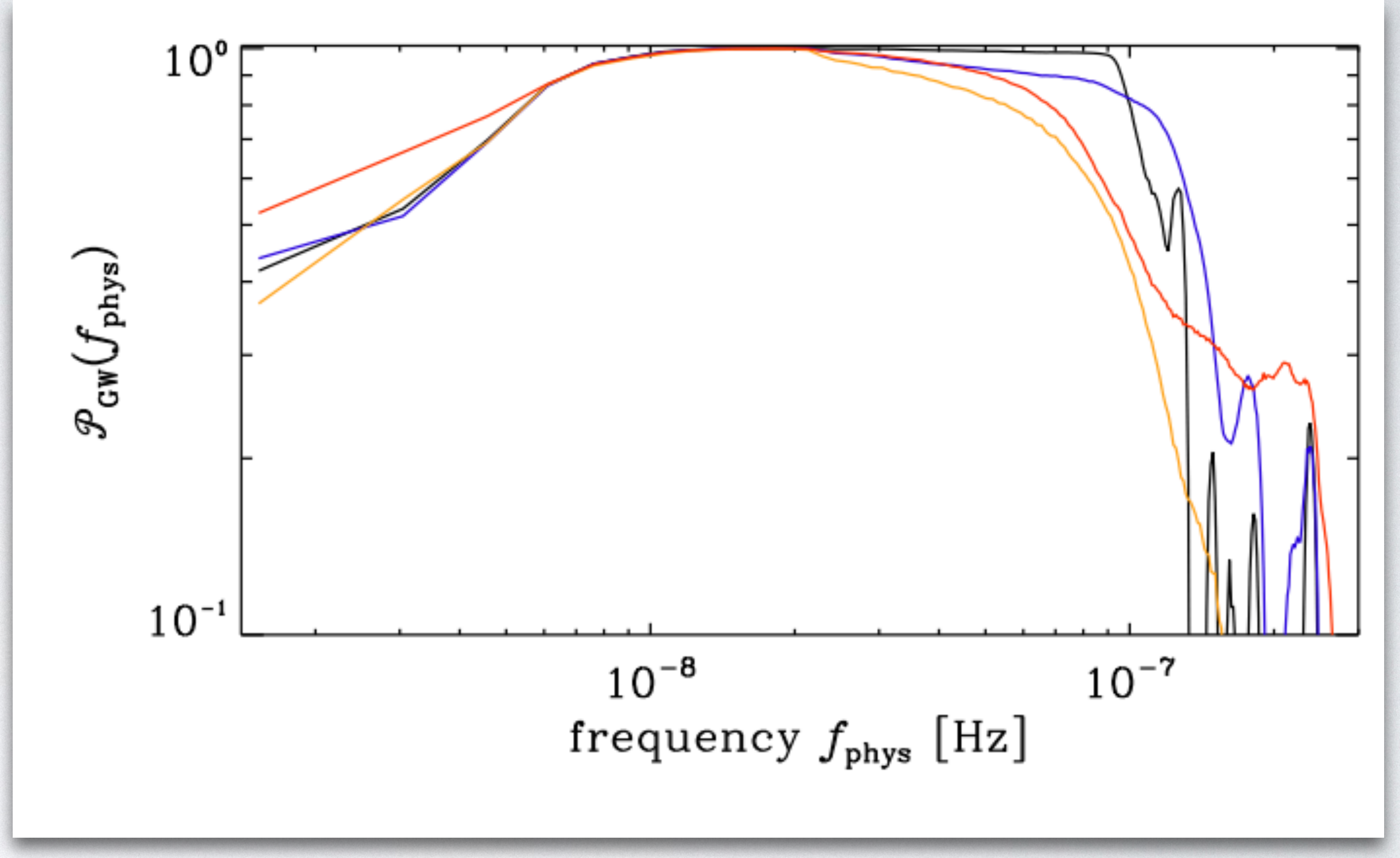

Run	f_0	ν
a	5×10^{-1}	2×10^{-2}
a2	3×10^{-1}	2×10^{-2}
b	3×10^{-1}	5×10^{-3}
c	2×10^{-1}	5×10^{-3}
d	1×10^{-1}	5×10^{-3}

CONCLUSIONS

- **Magnetic stress from hydrodynamic and MHD turbulence** with scales comparable to the cosmological horizon scale at the QCD transition **can drive GWs in the range accessible to existing detectors** including PTAs and astrometric missions.

- **GW spectrum observation could constrain the nature of the underlying turbulence in the early universe.**

  - The **peak** (amplitude and frequency) of the GW energy density is related to the maximum magnetic energy density and the wave number of the turbulent forcing.

  - **Below the break frequency**, the GW spectrum from QCD scale parameters is *shallower* in the non-helical case than helical ($\sim f^{1/2}$ vs $\sim f$) and both scalings are shallower than what was expected based on earlier analytical calculations.

  - **Above the peak frequency**, the GW spectrum has a sharp drop.

- **GW polarization** degree is determined by the helical properties of the source and could provide information about magnetogenesis and parity violation at the time of generation.

THANK YOU

SUPPLEMENTARY SLIDES

GW POLARIZATION SPECTRA

circular polarization degree

$$\mathcal{P}(k) = \frac{\left\langle h_+^*(\mathbf{k})h_+(\mathbf{k}') - h_-^*(\mathbf{k})h_-(\mathbf{k}')\right\rangle}{\left\langle h_+^*(\mathbf{k})h_+(\mathbf{k}') + h_-^*(\mathbf{k})h_-(\mathbf{k}')\right\rangle} = \frac{\mathcal{H}(k)}{H(k)}$$

- $\left\langle h_{ij}^*(\mathbf{k})h_{lm}(\mathbf{k}')\right\rangle/(2\pi)^3 = \delta^{(3)}(\mathbf{k}-\mathbf{k}')\left[\mathcal{M}_{ijlm}H(k) + i\mathcal{A}_{ijlm}\mathcal{H}(k)\right]$
- Retains information about the initial fractional helicity of source (Kahniashvili et al. 2021)

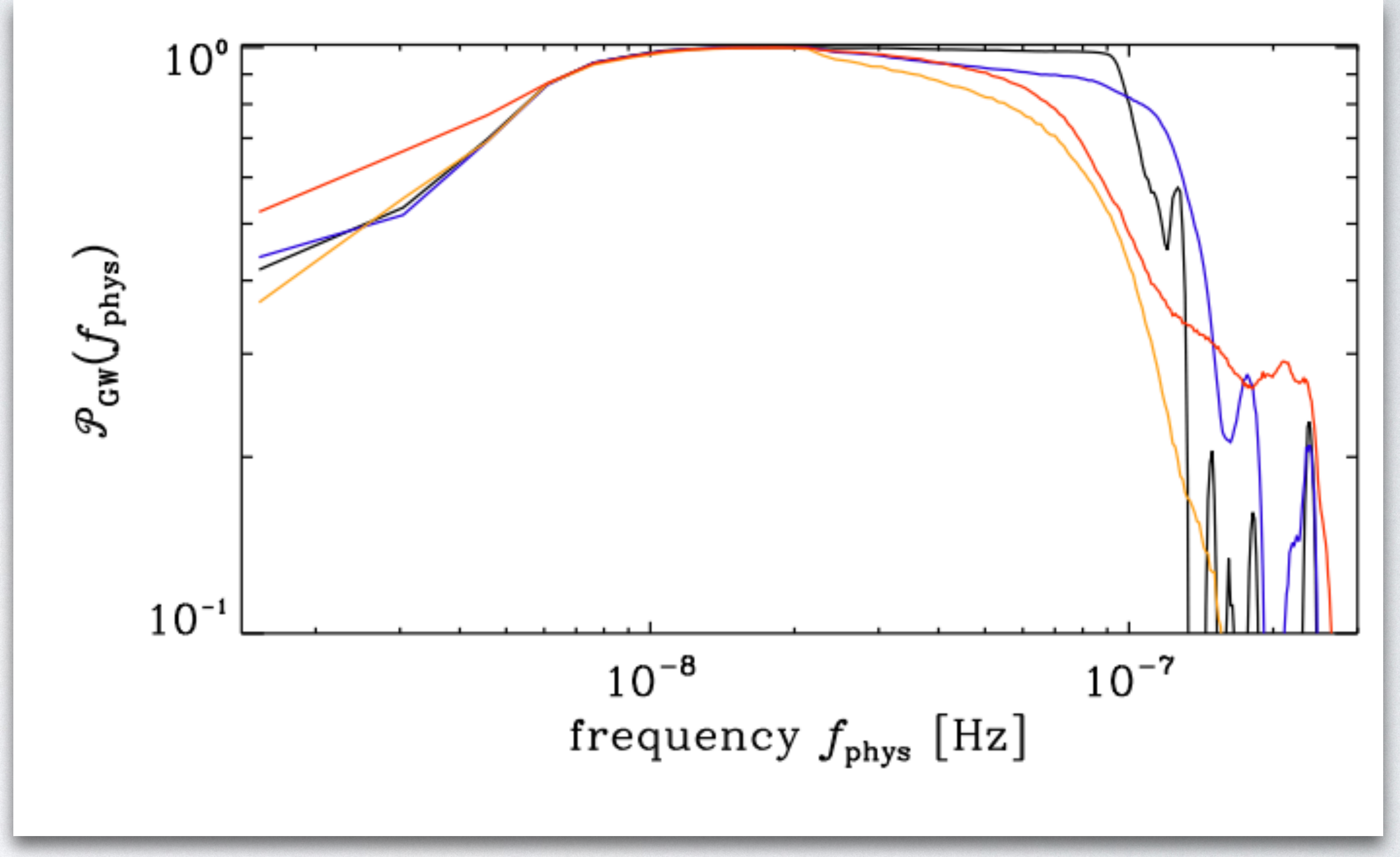

Run	f_0	ν
a	5×10^{-1}	2×10^{-2}
a2	3×10^{-1}	2×10^{-2}
b	3×10^{-1}	5×10^{-3}
c	2×10^{-1}	5×10^{-3}
d	1×10^{-1}	5×10^{-3}

MAGNETIC VS HYDRODYNAMIC TURBULENCE

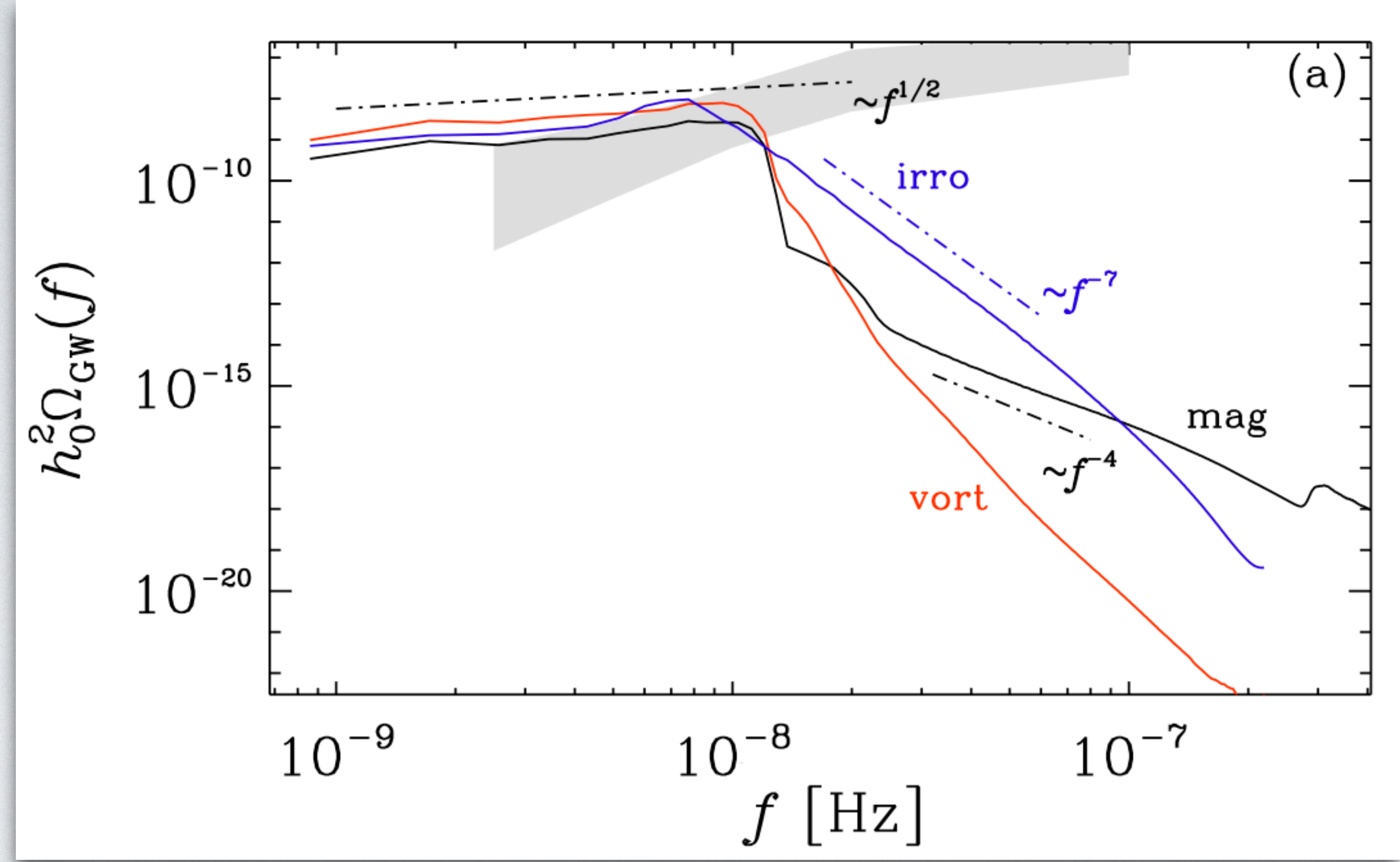

- MHD turbulence
  - vortical, non helical (`mag')
  - $\tau = (v_A k_f)^{-1}$ with $v_A = \sqrt{3\mathcal{E}_M/2}$ and $\mathcal{E}_M = \langle \mathbf{B}^2 \rangle/2$
- Hydrodynamic turbulence
  - vortical (divergence-free) forcing (`vort')
  - irrotational (curl-free) forcing (`irro')
  - $\tau = (u_{\rm rms} k_f)^{-1}$ with $u_{\rm rms} = \sqrt{2\mathcal{E}_K}$ and $\mathcal{E}_K = \langle \rho \mathbf{u}^2 \rangle/2$

Type	f_0	ν	$\mathcal{E}_M^{\rm max}$	$\mathcal{E}_{\rm GW}^{\rm sat}$	$h_{\rm rms}^{\rm sat}$	B [μG]	$h_0^2\Omega_{\rm GW}(f)$	h_c
magnetic	1.9×10^{-1}	5.0×10^{-5}	3.83×10^{-2}	3.53×10^{-4}	4.83×10^{-2}	0.78	1.09×10^{-8}	4.83×10^{-14}
vortical	3.8×10^{-1}	1.0×10^{-2}	4.21×10^{-2}	8.81×10^{-4}	8.26×10^{-2}	0.82	2.73×10^{-8}	8.27×10^{-14}
irrotational	7.0×10^{-1}	2.0×10^{-2}	4.26×10^{-2}	8.30×10^{-4}	7.95×10^{-2}	0.83	2.57×10^{-8}	7.96×10^{-14}

AXION MAGNETOGENESIS

Miniati et al 2018

$$
\begin{aligned}
\nabla \cdot \mathbf{E} &= \rho + \frac{g_{a\gamma}}{R^{3/2}} \mathbf{B} \cdot \nabla a, \\
\nabla \cdot \mathbf{B} &= 0, \\
\nabla \times \mathbf{B} &= \mathbf{J} + R \frac{\partial \mathbf{E}}{\partial t} + \\
& \frac{g_{a\gamma}}{R^{3/2}} \left[\mathbf{E} \times \nabla a - R\mathbf{B} \left(\frac{\partial a}{\partial t} - \frac{3}{2} \frac{\dot{R}}{R} a \right) \right] \\
\nabla \times \mathbf{E} &= -R \frac{\partial \mathbf{B}}{\partial t},
\end{aligned}
$$

- Consider a *smooth* QCD crossover
  - pressure gradients result from different charge density, energy density, and equation of state of the quark and lepton components
    - thermoelectric fields arise at pressure gradients
      - magnetic field may be generated by interaction of thermoelectric field with a pseudo-scalar axion field
- Axion coupling to the electromagnetic field (via Primakoff mechanism)
    - Lagrangian term: $\mathscr{L}_{\text{int}} = -g_{a\gamma} \mathbf{E} \cdot \mathbf{B} a$ where $g_{a\gamma}$ is the axion-photon coupling (depends on the specific axion model considered), *a* is the axion field
- Write Maxwell's equations in comoving coordinates considering this term:
- thermoelectric field arises at pressure gradients in the primordial plasma due to a slight asymmetry in the charge, energy density, and EoS of the quark and leptonic components $\mathbf{E} = \eta_p \mathbf{J} - \epsilon \frac{\nabla P}{en}$
    - Take 0 initial magnetic field: Ohm's law (where η_p is the coming plasma resistivity , $P = 7\pi^2 g^* R^4 T^4 / 720$ the comoving pressure with g* the relativistic degrees of freedom and $n = 3\zeta(3) g^* R^3 T^3 / 4\pi^2$ the coming density, ϵ accounts for the strength of the field only being a fraction of the usual baroclinic term)
- Ampere's Law (again with 0 initial magnetic field) yields: $\mathbf{J} \approx -\frac{g_{a\gamma}}{R^{3/2}} (\mathbf{E} \times \nabla a)$
- Substitute result for current into Ohm's law to find: $\mathbf{E} = -\frac{\mathcal{A}(\mathcal{A} \cdot \mathcal{H}) + \mathcal{A} \times \mathcal{H} + \mathcal{H}}{1 + \mathcal{A}^2}$ $\quad \mathcal{A} = \eta_p \frac{g_{a\gamma}}{R^{3/2}} \nabla a, \quad \mathcal{H} = \epsilon \frac{\nabla P}{en}$
- *If the axion field gradient and the thermoelectric field are not exactly aligned, an electric current is driven in the primordial plasma through their interaction.*
- **Magnetic seed field generated** in this process
- Pressure gradient that gives rise to the thermoelectric fields will generally ***drive large scale plasma motion***
    - initiates turbulent cascade which can lead to significant *amplification of the initial seed* by turbulent dynamo action

GW DETECTION

- PTAs in nHz range:
  - NANOGrav: 1 nHz - 1μHz
  - SKA (Square Kilometer Array)
  - EPTA
- Ground-based interferometers:
  - aLIGO: 10 Hz - 1000 Hz
  - ET (proposed)
- (Future) Space-based Interferometers:
  - LISA: 0.1 mHz - 1 Hz
  - DECIGO: 0.1 Hz - 10 Hz
- Astrometry: GAIA + THEIA: nHz range (between PTA and LISA)

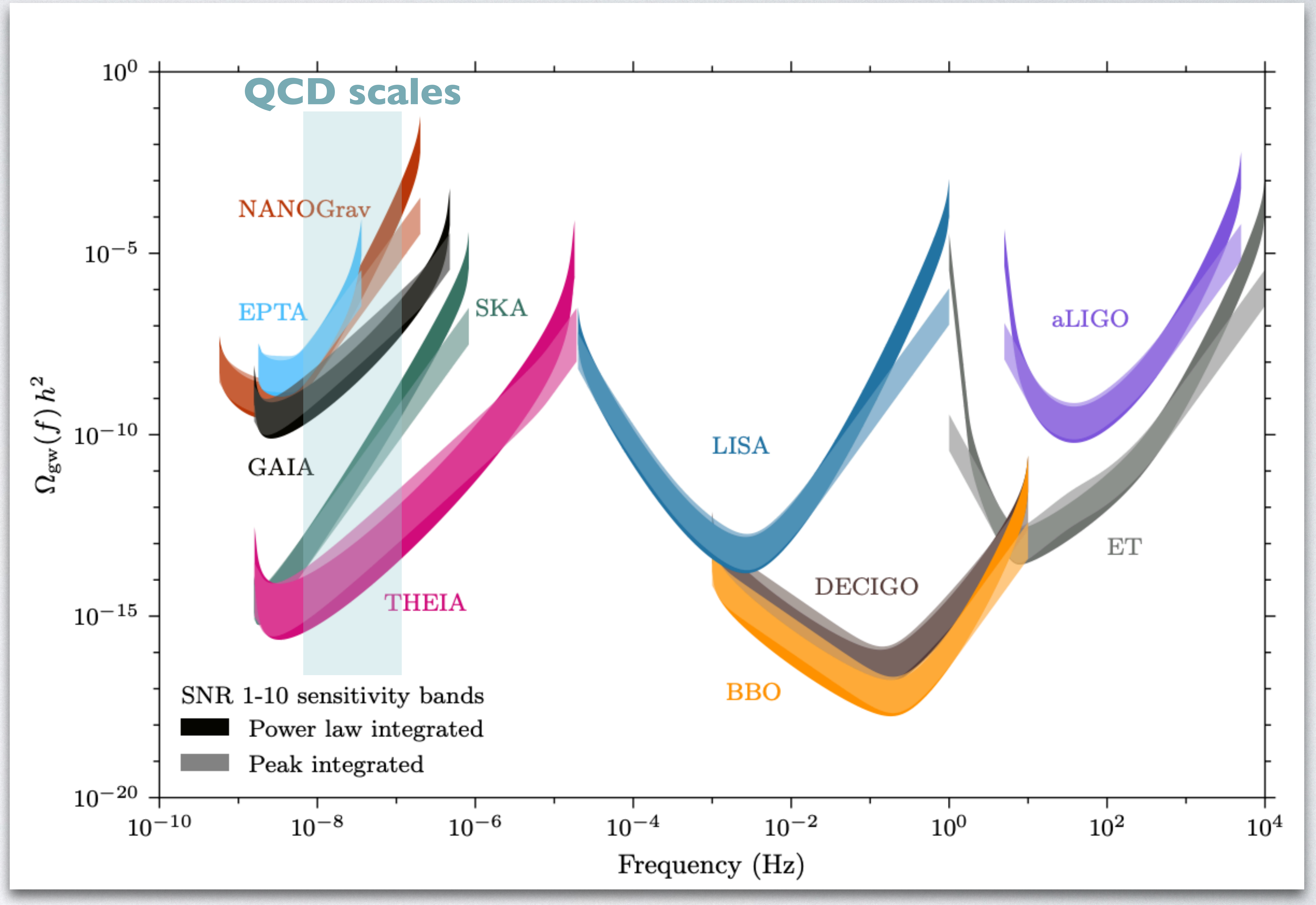

Garcia-Bellido, Murayama, White (2021)

ENERGY DENSITY

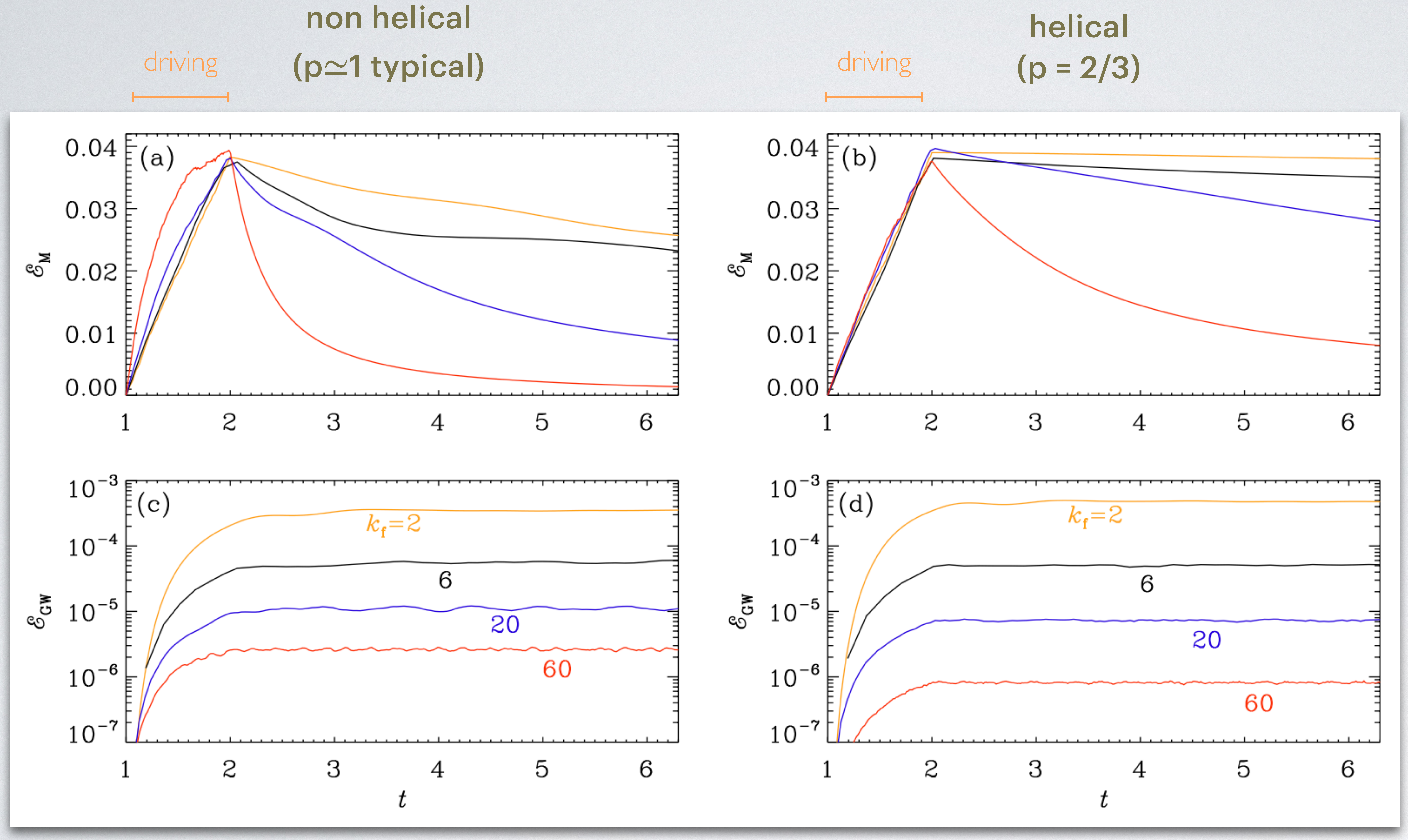

magnetic energy density

$$\mathcal{E}_M \sim \langle \mathbf{B}^2 \rangle$$

peak value $\mathcal{E}_M^{max}$

turbulent decay

$$\mathcal{E}_M(t) \sim t^{-p}$$

energy density carried by GWs

$$\mathcal{E}_{GW} \sim \langle \dot{h}^2 \rangle$$

saturates at $\mathcal{E}_{GW}^{sat}$

$$\mathcal{E}_{GW}^{sat} = (q\mathcal{E}_M^{max}/k_f)^2$$

with $q = 1.1$

MAGNETIC FIELD EVOLUTION

- Initial Conditions of Magnetic Field
  - Generated at time η_*
  - Strength B_* BBN upper limit
  - Maximum correlation length $\xi_{M*} \leq \lambda_{H*}$ (Hubble horizon)
- Scaling Exponents: p, q
  - depend on the properties of the turbulence
  - determined/verified by numerical simulations (Brandenburg & Kahniashvili 2017)
  - $p = (\beta + 1)\, q$
- Fractional helicity: ratio of the magnetic helicity to its maximal value

$$\epsilon_M(\eta) = \frac{\xi_M^{\min}(\eta)}{\xi_M(\eta)} = \frac{\mathscr{H}_M(\eta)}{2\xi_M(\eta)\mathscr{E}_M(\eta)} \leq 1$$

- Evolution

$$\xi_M = \xi_{M*}\left(\frac{\eta}{\eta_*}\right)^{q} \qquad B = B_*\left(\frac{\eta}{\eta_*}\right)^{-p/2}$$

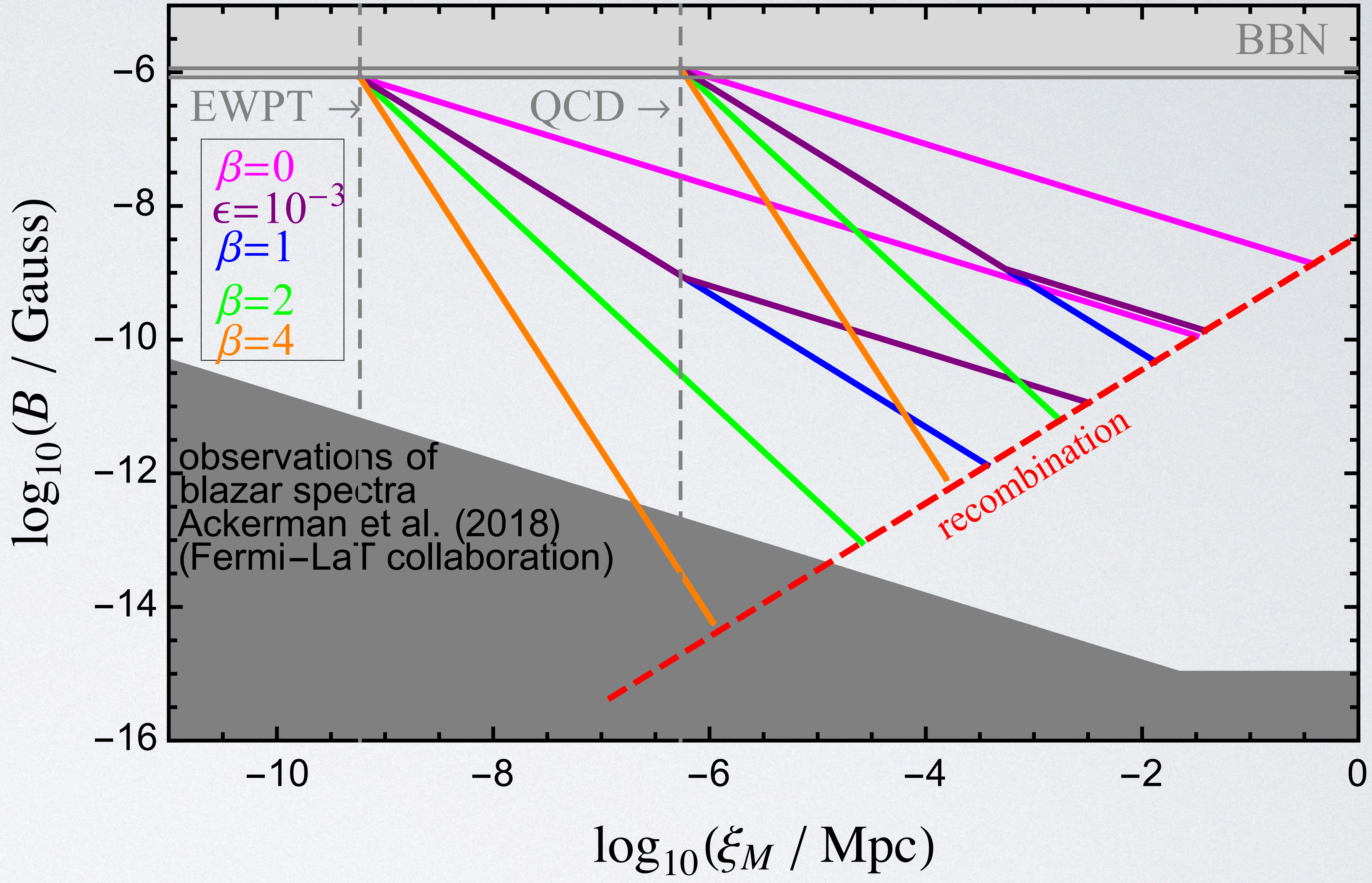

	p	q, n_ξ
fully helical (β=0)	2/3	2/3
nonhelical (β=1)	1	1/2
nonhelical (β=2)	6/5	2/5
nonhelical (β=4)	10/7	2/7

MAGNETIC FIELD EVOLUTION

- Initial Conditions of Magnetic Field
    - Generated at time η_*
    - Strength ~~B_* BBN upper limit~~
    - Maximum correlation length $\xi_{M*} \leq \lambda_{H*}$ (Hubble horizon)
- Scaling Exponents: p, q
    - depend on the properties of the turbulence
    - determined/verified by numerical simulations (Brandenburg & Kahniashvili 2017)
    - $p = (\beta + 1)\, q$
- Fractional helicity: ratio of the magnetic helicity to its maximal value

$$\epsilon_M(\eta) = \frac{\xi_M^{\min}(\eta)}{\xi_M(\eta)} = \frac{\mathscr{H}_M(\eta)}{2\xi_M(\eta)\mathscr{E}_M(\eta)} \leq 1$$

- Evolution

$$\xi_M = \xi_{M*}\left(\frac{\eta}{\eta_*}\right)^{q} \qquad\qquad B = B_*\left(\frac{\eta}{\eta_*}\right)^{-p/2}$$

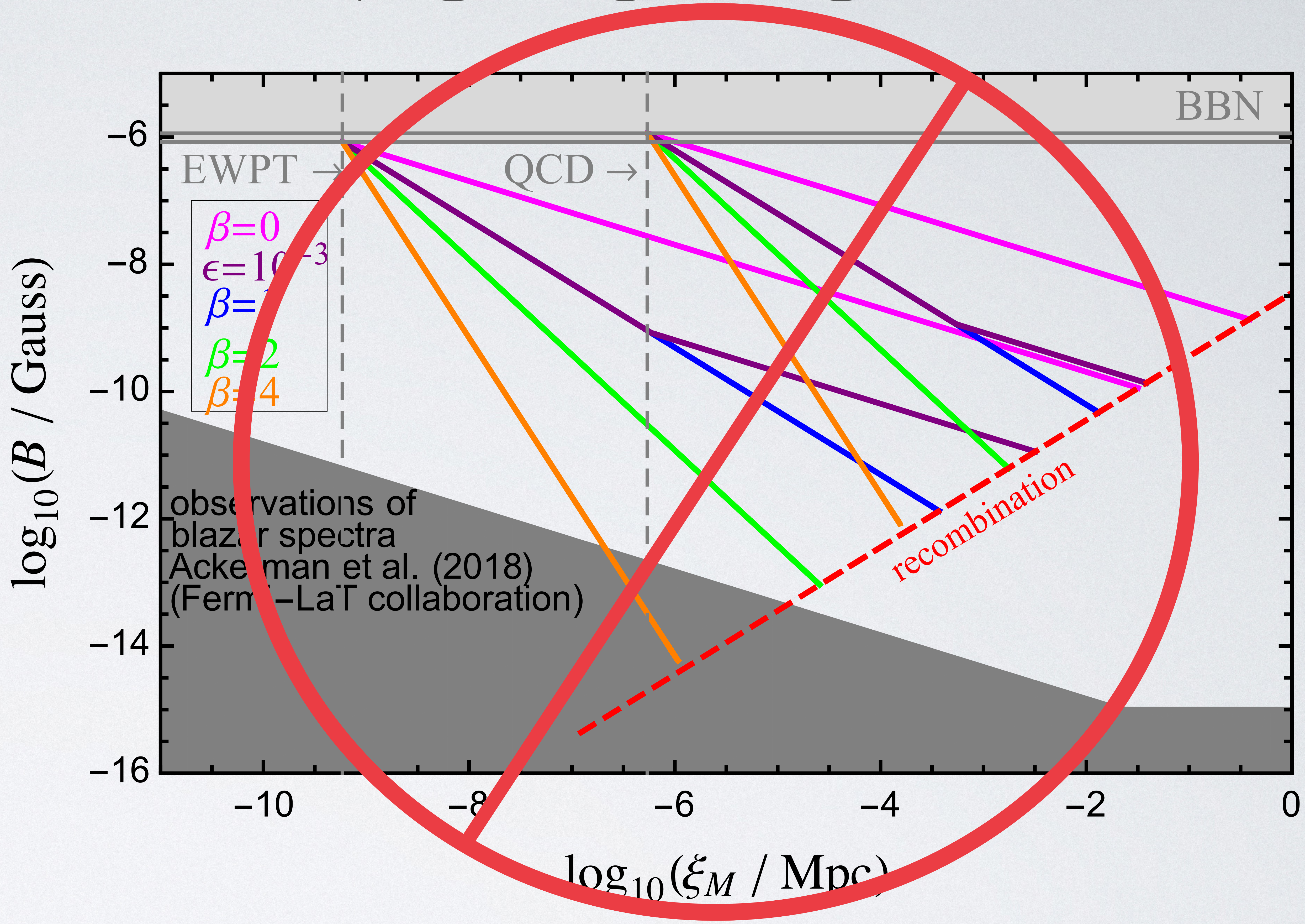

	p	$q,\ n_\xi$
fully helical (β=0)	2/3	2/3
nonhelical (β=1)	1	1/2
nonhelical (β=2)	6/5	2/5
nonhelical (β=4)	10/7	2/7

TURBULENT EVOLUTION WITH UPDATED BBN BOUNDS

- <u>New bounds</u>: apply BBN bound *at BBN* $T_{\rm BBN}$
  - Field strength decays $B \sim t^{-p/2}$
- Correlation length grows $\xi_M \sim t^q$
  - Maximum correlation length $\xi_{M*} \leq \lambda_{H*}$ (Hubble horizon)
  - consider up to 6 at QCD
- Trajectories end at recombination (0.25 eV)
- $p = (\beta + 1)\, q$
- β, p, q depend on on turbulence properties
- fractional helicity:

$$\epsilon_M(\eta) = \frac{\xi_M^{\min}(\eta)}{\xi_M(\eta)} = \frac{\mathscr{H}_M(\eta)}{2\xi_M(\eta)\mathscr{E}_M(\eta)} \leq 1$$

	p	q, n_ξ
fully helical (β=0)	2/3	2/3
nonhelical (β=1)	1	1/2
nonhelical (β=2)	6/5	2/5
nonhelical (β=4)	10/7	2/7

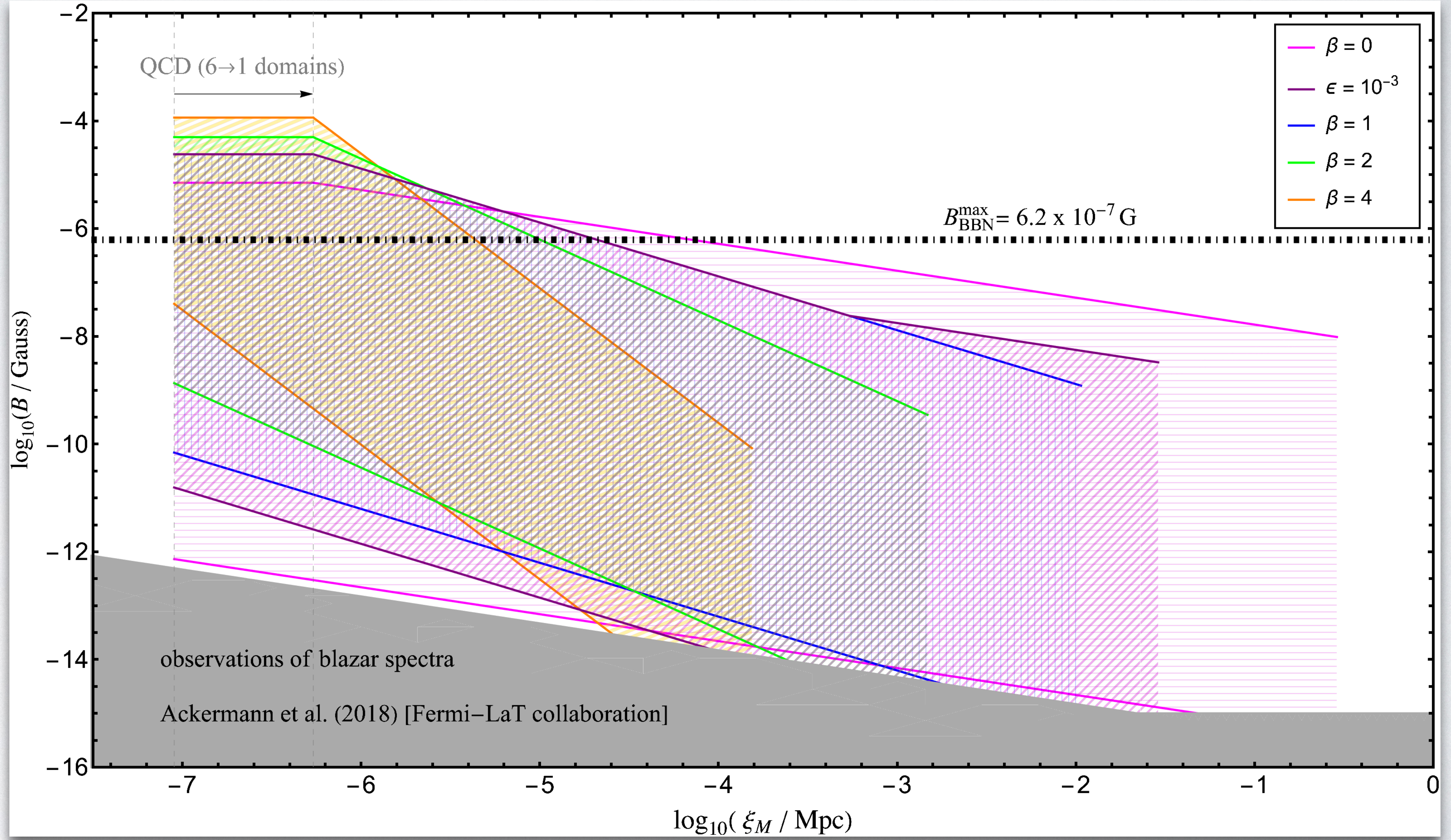

ENERGY DENSITY

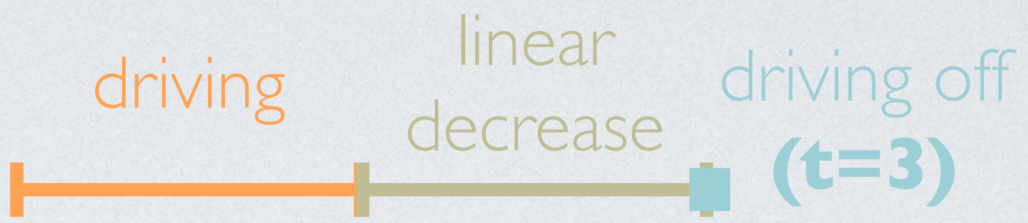

- EW scale: Runs A-D
  - forcing and viscosity decrease A→D
- QCD scale: Runs a-d

Run	f_0	ν
a	5×10^{-1}	2×10^{-2}
a2	3×10^{-1}	2×10^{-2}
b	3×10^{-1}	5×10^{-3}
c	2×10^{-1}	5×10^{-3}
d	1×10^{-1}	5×10^{-3}
A	7×10^{-3}	5×10^{-5}
A’	7×10^{-3}	5×10^{-5}
A2	7×10^{-3}	1×10^{-4}
O1	5×10^{-3}	5×10^{-5}
O1’	5×10^{-3}	5×10^{-5}
O2	5×10^{-3}	1×10^{-4}
B	2×10^{-3}	2×10^{-6}
C2	1×10^{-3}	2×10^{-6}
C	1×10^{-3}	2×10^{-7}
D	6×10^{-4}	2×10^{-7}

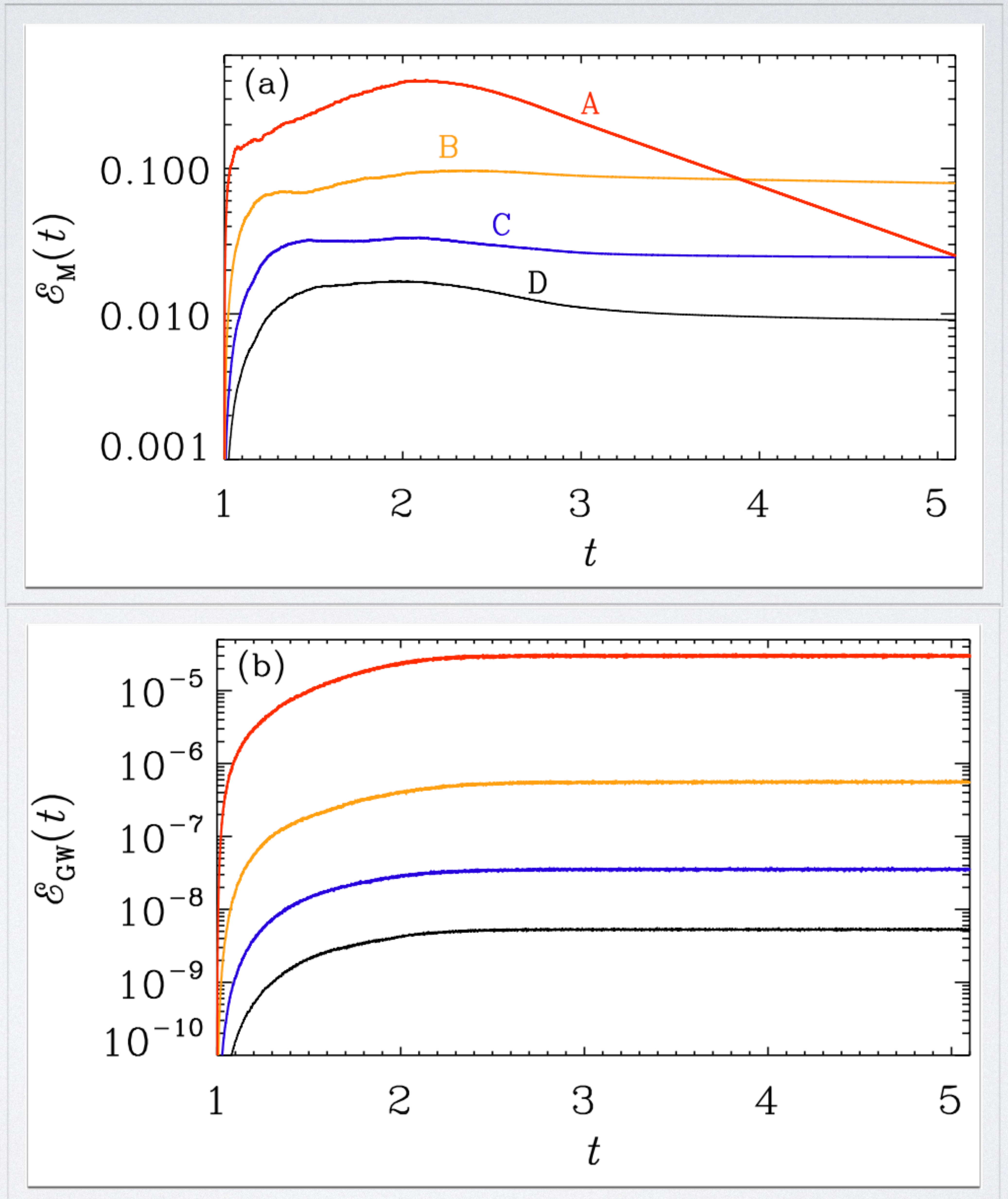

magnetic energy density

$$\mathcal{E}_{\mathrm{M}} \sim \langle \mathbf{B}^2 \rangle$$

peak value $\mathcal{E}_{\mathrm{M}}^{\mathrm{max}}$

turbulent decay

$$\mathcal{E}_{\mathrm{M}}(t) \sim t^{-p}$$

energy density carried by GWs

$$\mathcal{E}_{\mathrm{GW}} \sim \langle \dot{h}^2 \rangle$$

saturates at $\mathcal{E}_{\mathrm{GW}}^{\mathrm{sat}}$

$$\mathcal{E}_{\mathrm{GW}}^{\mathrm{sat}} = (q\mathcal{E}_{\mathrm{M}}^{\mathrm{max}}/k_{\mathrm{f}})^2$$

with $q = 1.1$